

The analysis of the channel flow sensitivity to the parameters of the k – ε method

Ewa Błazik-Borowa^{*,†}

Faculty of Civil and Sanitary Engineering, Department of Structural Mechanics, Lublin University of Technology, ul. Nadbystrzycka 40, 20-618 Lublin, Poland

SUMMARY

This paper deals with the problem of using sensitivity analysis for fluid mechanics solutions to the constants of the standard k – ε method for 2D, incompressible and steady flows. The problem is described and analysed on the basis of a channel flow. Sensitivity coefficients of the following properties were determined: a pressure, two components of a velocity, a turbulence kinetic energy, a dissipation rate of turbulence kinetic energy and a turbulence dynamic viscosity. The calculated property values depend on five model constants that are parameters of the sensitivity analysis in this paper. Sensitivity coefficients are derivatives of the above properties, for individual parameters. In this paper these coefficients are determined using a finite difference approximation to the sensitivities coefficients.

The author of this paper compares three models of the boundary layer with regard to the sensitivity of properties to the parameters. Irrespective of the boundary layer model used here, the analysis of sensitivity coefficients for the channel flow properties shows that the most sensitive property is the turbulence dissipation rate. Next properties of consequence, although of significantly smaller values of sensitivity coefficients, are the turbulence viscosity and the turbulence kinetic energy. All flow properties are mostly sensitive to the C_μ parameter. One of the final conclusions in this paper is that the analysis of sensitivity coefficient fields allows the reliable checking of results and indicates those areas most prone to calculation difficulties. Copyright © 2008 John Wiley & Sons, Ltd.

Received 10 June 2007; Revised 22 February 2008; Accepted 23 February 2008

KEY WORDS: plane channel flow; k – ε turbulence model; sensitivity analysis

1. INTRODUCTION

The k – ε model is often used to model turbulence of a flow in computational fluid dynamics problems. The application of this method to obtain correct results requires the evaluation of semi-empirical coefficients for the model. These coefficients are called ‘constants’ in the literature.

*Correspondence to: Ewa Błazik-Borowa, Faculty of Civil and Sanitary Engineering, Department of Structural Mechanics, Lublin University of Technology, ul. Nadbystrzycka 40, 20-618 Lublin, Poland.

†E-mail: e.blazik-borowa@pollub.pl, e.blazik@pollub.pl

Numerous versions of this model have been developed since the 1970s, when the standard version model was popularized by Launder and Spalding (comp. [1, 2]) and others. Unfortunately, the new turbulence models of the $k-\varepsilon$ type also include ‘constants’ calibrated on the basis of measurements, theoretical analyses and the experience of the computer program users. The largest number of papers concerning the $k-\varepsilon$ model were written in the 1990s. In spite of the fact that turbulence models based on the LES method are currently being developed, $k-\varepsilon$ turbulence models are still in common use within commercial programs. As users of the $k-\varepsilon$ turbulence model know its constraints, they are able to avoid them. It is anticipated, therefore, that the new flow modelling methods (such as LES or DVM) will be an alternative to the $k-\varepsilon$ method for as long as research devoted to adjusting the old method to new issues remains useful. On the other hand, over 10 different sets of values for these ‘constants’ may be found in the literature (comp. [3, 4]), indicating that the selection of ‘constants’ is still a serious problem. This is one of the reasons why using sensitivity analysis to check the influence of the selection of ‘constants’ for the $k-\varepsilon$ model has been presented in this paper. As ‘constants’ of the $k-\varepsilon$ model are not constant and they are input data of the sensitivity analysis, they are called parameters of the $k-\varepsilon$ model in this paper.

This paper consists of two parts. The first part includes a description of methods used in order to obtain the sensitivity coefficients, whereas the second part presents the results of the sensitivity analysis for the channel flow that will be used to check the method of modelling the boundary layer with the FLUENT program, paying special attention to reliability of the turbulence model parameters (constants) used. The method discussed will be presented with the example of the standard of the $k-\varepsilon$ model for steady incompressible flows in a channel.

2. THE $k-\varepsilon$ TURBULENCE MODEL

2.1. Equations and parameters for the $k-\varepsilon$ model

The sensitivity analysis problems will be presented on the basis of the standard $k-\varepsilon$ turbulence model (comp. [1, 2] and others) for the channel flow that is treated as incompressible fluids. In this method, flow properties may be described with the following system of differential equations:

- continuity equation:

$$\nabla \cdot \mathbf{u} = 0 \quad (1)$$

- Navier–Stokes equation:

$$\rho \left(\frac{\partial}{\partial t} \mathbf{u} + (\mathbf{u} \cdot \nabla) \mathbf{u} \right) = -\nabla p + (\mu + \mu_t) \Delta \mathbf{u} \quad (2)$$

- turbulence kinetic energy equation:

$$\rho \left(\frac{\partial k}{\partial t} + (\mathbf{u} \cdot \nabla) k \right) = \left(\nabla \frac{\mu_t}{\sigma_k} \right) \cdot (\nabla k) + \frac{\mu_t}{\sigma_k} \Delta k + \rho P_k - \rho \varepsilon \quad (3)$$

- dissipation rate of the turbulence kinetic energy equation:

$$\rho \left(\frac{\partial \varepsilon}{\partial t} + (\mathbf{u} \cdot \nabla) \varepsilon \right) = \left(\nabla \frac{\mu_t}{\sigma_\varepsilon} \right) \cdot (\nabla \varepsilon) + \frac{\mu_t}{\sigma_\varepsilon} \Delta \varepsilon + \rho C_{\varepsilon 1} P_k \frac{\varepsilon}{k} - \rho C_{\varepsilon 2} \frac{\varepsilon^2}{k} \quad (4)$$

- equation of the turbulence dynamic viscosity:

$$\mu_t = \rho C_\mu \frac{k^2}{\varepsilon} \quad (5)$$

where p is the pressure, $\mathbf{u} = [u_1 \ u_2 \ u_3]^T$ is the velocity vector, k is the turbulence kinetic energy, ε is the dissipation of a turbulence kinetic energy, μ_t is the turbulence dynamic viscosity, t is the time, $\rho = 1.225 \text{ kg/m}^3$ is the air density, $\mu = 2.192 \times 10^{-5} \text{ Ns/m}^2$ is the dynamic viscosity, $\nabla = [\partial/\partial x_1 \ \partial/\partial x_2 \ \partial/\partial x_3]$ is the Hamilton operator, $\Delta = \nabla^2 = \partial^2/\partial x_1^2 + \partial^2/\partial x_2^2 + \partial^2/\partial x_3^2$ is the Laplace operator, $\rho P_k = \mu_t S^2$ is the turbulence energy production, S is the modulus of the mean rate-of-strain tensor, defined as $S \equiv \sqrt{2s_{ij}s_{ij}}$ and $s_{ij} = 1/2(\partial u_i/\partial x_j + \partial u_j/\partial x_i)$, and $C_{\varepsilon 1}$, $C_{\varepsilon 2}$, C_μ , σ_k and σ_ε are the parameters of the k - ε model.

According to the assumptions of the k - ε turbulence method, flow properties present in the system of equations are time-averaged values. The above equations were obtained using the simplifying assumptions: Reynolds averaging, Boussinesq hypothesis, Prandtl hypothesis based on the Ficks law [5] and Kolmogorows hypothesis of the turbulence local isotropy [6]. The effect of introducing these hypotheses is the presence of the model parameters in the equations. Although in the literature these parameters are called ‘constants’, their values are adjusted to different problems. The calibration of the parameters has been described by Bottema [7], Comte-Bellot and Corrsin [8], Hrenya *et al.* [3], Launder and Spalding [1, 2], Shih [9] and many others. Nowadays, the most frequently used set of parameter values is as follows: $C_\mu = 0.09$, $C_{\varepsilon 1} = 1.44$, $C_{\varepsilon 2} = 1.92$, $\sigma_k = 1.0$ and $\sigma_\varepsilon = 1.3$. They are also the values of parameters recommended by FLUENT, whose results will be presented below. In order to show that the sensitivity analysis of the flow properties to model parameters is necessary, the bases for the calibration of each value are described below.

This short description of the calibration method will start with the C_μ parameter. This quantity is based on the assumption of equilibrium between the turbulence energy production and the turbulence dissipation rate near the walls. According to Launder and Spalding [1], this value is included in the range $C_\mu \in (0.0625; 0.09)$. Yet, Shih [9] gave values in the range from $C_\mu = 0.05$ (with homogeneous flow away from the wall) to $C_\mu = 0.09$ (at flat wall), and Bottema [7] suggested even smaller value for atmospheric flows, i.e. $C_\mu = 0.03$, in the atmospheric turbulence conditions.

Another $C_{\varepsilon 1}$ parameter describes a relationship between dissipation production and turbulence energy production. The $C_{\varepsilon 1}$ parameter is determined based on fairly complicated measurements, preferably taken in the boundary layer, and the results of which should be the turbulence kinetic energy, the dissipation rate and the components of strain rate tensor. In papers [3, 4, 10, 11] developing the problem of calculations made with the k - ε model, the $C_{\varepsilon 1}$ parameter is between 1.15 and 1.5.

If the isotropic homogeneous turbulence (for high Reynolds numbers) is assumed, the average stress field and diffusion disappear (comp. [12]) and the kinetic energy and dissipation rate equations (comp. Equations (3) and (4)) are reduced to simple differential equations:

$$\frac{dk}{dt} = -\varepsilon \quad (6)$$

$$\frac{d\varepsilon}{dt} = -C_{\varepsilon 2} \frac{\varepsilon^2}{k} \quad (7)$$

The following equation is the solution to the above system of equations (comp. [13]):

$$k(t) = k_0 \left\{ 1 + (C_{\varepsilon 2} - 1) \frac{\varepsilon_0}{k_0} t \right\}^{-n} \quad (8)$$

where

$$n = \frac{1}{C_{\varepsilon 2} - 1} \quad (9)$$

The n value is obtained from the measurements of changes in the turbulence kinetic energy over time for high Reynolds number. Comte-Bellot and Corrsin [8] obtained values of n between 1.2 and 1.3, whereas Mohamed and Larue [14] obtained values between 1.08 and 1.3. In relation to the second, larger range, the $C_{\varepsilon 2}$ parameter assumes the values $C_{\varepsilon 2} \in (1.77; 1.93)$, whereas other literature mentions values for this parameter between 1.68 (comp. [11]) and 2.0 (comp. [15]).

The following paragraphs will describe the σ_k and σ_ε parameters, known as Schmidt (Prandtl) numbers. Launder and Spalding [1] performed a detailed analysis of this quantity, based on measurements. Graphs presented in their papers reveal that σ_k assumes values between 0.5 (in the free stream) and 1.75 (near the wall). In relation to some flows, e.g. pipe flows, the values fluctuate between 0.7 and 1.0, depending on the Reynolds number. There is also a relationship between the Schmidt number σ_k and a flow velocity. It is possible to state that σ_k is smaller at smaller velocities. Nevertheless, Launder and Spalding [1] gave its most probable value at $\sigma_k = 1.0$, although in the literature numbers between 0.61 and 1.36 are mentioned.

The Schmidt number σ_ε calibration is done in relation to the flow near the wall and is based on the assumption that velocity changes according to the following logarithmic function in this area:

$$\frac{u_t}{u_\tau} = \frac{1}{\kappa} \ln \left(E \frac{u_\tau}{\nu} y \right) \quad (10)$$

where $\kappa = 0.4187$ is the Kármán constant, $E = 9.81$ is the empirical constant, u_t is the component of velocity along the wall, u_τ is the shear velocity, y is the distance to the wall and ν is the kinetic viscosity.

The following equation is obtained through the use of many reductions, including those that contain approximate dimensionless relationships between quantities proportional to each other:

$$\sigma_\varepsilon = \frac{\kappa^2 / \sqrt{C_\mu}}{(C_{\varepsilon 2} - C_{\varepsilon 1})} \quad (11)$$

The above equation includes most of the k - ε model parameters. The value of σ_ε depends largely on their evaluation, which is often made on the basis of measurements. Bottema [7], on the

basis of his literature studies, claims that $\sigma_\varepsilon \in (1.3; 2.38)$, but smaller values, such as 0.75, are suggested.

It is notable that the span of the $C_{\varepsilon 1}$, $C_{\varepsilon 2}$, C_μ , σ_k and σ_ε values is very large, and hence calling them ‘constants’ is rather doubtful. For that reason, the term ‘constants’ is replaced by parameters in this paper and the quantities are treated as variables of functions describing the flow properties. This may allow the determining of derivatives for the properties in relation to the parameters, i.e. determining sensitivity coefficients.

2.2. Boundary layer models

In the second part of this paper, the results of sensitivity analyses of problems solved using FLUENT 6.1.18 will be compared with each other. Three methods of modelling the boundary layer will be used for solving the problems:

- boundary layer model no. 1 in which the flow velocity is described by Equation (10) and the dissipation rate by the following:

$$\varepsilon = \frac{C_\mu^{3/4} k^{3/2}}{\kappa x_n} \quad (12)$$

an equilibrium between the production and the dissipation rate is assumed; these assumptions are used for the first layer of volumes nearest the wall;

- boundary layer model no. 2 in which a velocity profile is assumed to be similar to model no. 1 but the assumption of equilibrium between the production and the dissipation rate of the turbulence kinetic energy is omitted;
- boundary layer model no. 3 in which the value of Reynolds number Re is checked for each volume; if $Re < 200$, the single-equation Wolfstein model [16] is used to describe the flow movement; if $Re > 200$, the whole $k-\varepsilon$ turbulence model is used.

3. SENSITIVITY ANALYSIS

The sensitivity analysis is a method used to examine the influence of changing input parameters on results. To date it has been widely used in solid mechanics and in structural mechanics (comp. [17]), but recently it has been used in fluid mechanics as well, e.g. for examining the influence of the geometric parameters of pipes on flow properties (comp. [18]), and as a tool for considering the cooperation of a moving body and the fluid surrounding it [19]. In this paper, the sensitivity analysis is used to examine how changing the parameters of the $k-\varepsilon$ model influences the calculation results of the flow. The manner of application of the sensitivity analysis was created by the author [20] and the group of Pelletier (comp. Colin *et al.* [21]) at the same time, but Pelletier with collaborators published their results first.

It is worth remembering that the flow may be described with the following property fields: the pressure p , the velocity components u_1, u_2, u_3 (two in 2D problems and three in 3D problems), the turbulence kinetic energy k , the turbulence dissipation rate ε and the turbulence dynamic viscosity μ_t . The determination of flow properties will be called the main problem. At the same time, in (1)–(5) model equations for the standard $k-\varepsilon$ model (in which buoyancy and temperature are not taken into account) there are five parameters: $C_{\varepsilon 1}$, $C_{\varepsilon 2}$, C_μ , σ_k and σ_ε . The sensitivity of the properties to the parameters is derivatives, which may be set into the following matrix in relation

to one point of fields in a 2D problem:

$$\mathbf{J} = \begin{bmatrix} \tilde{p}_{C_{\varepsilon 1}} & \tilde{p}_{C_{\varepsilon 2}} & \tilde{p}_{C_{\mu}} & \tilde{p}_{\sigma_k} & \tilde{p}_{\sigma_{\varepsilon}} \\ \tilde{u}_{1C_{\varepsilon 1}} & \tilde{u}_{1C_{\varepsilon 2}} & \tilde{u}_{1C_{\mu}} & \tilde{u}_{1\sigma_k} & \tilde{u}_{1\sigma_{\varepsilon}} \\ \tilde{u}_{2C_{\varepsilon 1}} & \tilde{u}_{2C_{\varepsilon 2}} & \tilde{u}_{2C_{\mu}} & \tilde{u}_{2\sigma_k} & \tilde{u}_{2\sigma_{\varepsilon}} \\ \tilde{k}_{C_{\varepsilon 1}} & \tilde{k}_{C_{\varepsilon 2}} & \tilde{k}_{C_{\mu}} & \tilde{k}_{\sigma_k} & \tilde{k}_{\sigma_{\varepsilon}} \\ \tilde{\varepsilon}_{C_{\varepsilon 1}} & \tilde{\varepsilon}_{C_{\varepsilon 2}} & \tilde{\varepsilon}_{C_{\mu}} & \tilde{\varepsilon}_{\sigma_k} & \tilde{\varepsilon}_{\sigma_{\varepsilon}} \\ \tilde{\mu}_{C_{\varepsilon 1}} & \tilde{\mu}_{C_{\varepsilon 2}} & \tilde{\mu}_{C_{\mu}} & \tilde{\mu}_{\sigma_k} & \tilde{\mu}_{\sigma_{\varepsilon}} \end{bmatrix} = \begin{bmatrix} \frac{\partial p}{\partial C_{\varepsilon 1}} & \frac{\partial p}{\partial C_{\varepsilon 2}} & \frac{\partial p}{\partial C_{\mu}} & \frac{\partial p}{\partial \sigma_k} & \frac{\partial p}{\partial \sigma_{\varepsilon}} \\ \frac{\partial u_1}{\partial C_{\varepsilon 1}} & \frac{\partial u_1}{\partial C_{\varepsilon 2}} & \frac{\partial u_1}{\partial C_{\mu}} & \frac{\partial u_1}{\partial \sigma_k} & \frac{\partial u_1}{\partial \sigma_{\varepsilon}} \\ \frac{\partial u_2}{\partial C_{\varepsilon 1}} & \frac{\partial u_2}{\partial C_{\varepsilon 2}} & \frac{\partial u_2}{\partial C_{\mu}} & \frac{\partial u_2}{\partial \sigma_k} & \frac{\partial u_2}{\partial \sigma_{\varepsilon}} \\ \frac{\partial k}{\partial C_{\varepsilon 1}} & \frac{\partial k}{\partial C_{\varepsilon 2}} & \frac{\partial k}{\partial C_{\mu}} & \frac{\partial k}{\partial \sigma_k} & \frac{\partial k}{\partial \sigma_{\varepsilon}} \\ \frac{\partial \varepsilon}{\partial C_{\varepsilon 1}} & \frac{\partial \varepsilon}{\partial C_{\varepsilon 2}} & \frac{\partial \varepsilon}{\partial C_{\mu}} & \frac{\partial \varepsilon}{\partial \sigma_k} & \frac{\partial \varepsilon}{\partial \sigma_{\varepsilon}} \\ \frac{\partial \mu_t}{\partial C_{\varepsilon 1}} & \frac{\partial \mu_t}{\partial C_{\varepsilon 2}} & \frac{\partial \mu_t}{\partial C_{\mu}} & \frac{\partial \mu_t}{\partial \sigma_k} & \frac{\partial \mu_t}{\partial \sigma_{\varepsilon}} \end{bmatrix} \quad (13)$$

The sensitivity coefficients, such as the flow properties, make a field within the whole calculation area. A particular set (e.g. of 30 coefficients in 2D problems) of coefficient fields corresponds to a particular set of parameters.

The fields of the sensitivity coefficients may be determined using a finite difference approximation to the sensitivity coefficients or the forward sensitivity analysis. The finite difference approximation consists in calculating flows at the values next to the value of the parameter being analysed, and then determining the sensitivity coefficients with the following equation:

$$\tilde{s}_m = \frac{w_2 - w_1}{\Delta C_m} \quad (14)$$

where C_m is the examined parameter and w_1, w_2 are the results of calculations at $C_m - \Delta C_m/2$ and $C_m + \Delta C_m/2$, respectively. In further analyses, the ΔC_m increment is equal to one order bigger than the order of rounding the parameter in the main problem, it is $\Delta C_{\varepsilon 1} = \Delta C_{\varepsilon 2} = \Delta \sigma_k = \Delta \sigma_{\varepsilon} = 0.1, \Delta C_{\mu} = 0.01$.

The second method of determining the sensitivity coefficients consists in differentiating equations (1)–(5) describing the problem, with respect to the analysed parameter. Assuming that the model parameters do not depend on time for steady flow, after differentiating equations (1)–(5) in relation to the parameter marked as C_m , the following system of differential equations is obtained:

$$\nabla \cdot \tilde{\mathbf{u}}_m = 0 \quad (15)$$

$$\rho((\tilde{\mathbf{u}}_m \cdot \nabla)\mathbf{u} + (\mathbf{u} \cdot \nabla)\tilde{\mathbf{u}}_m) = -\nabla \tilde{p}_m + \tilde{\mu}_m \Delta \mathbf{u} + (\mu + \mu_t) \Delta \tilde{\mathbf{u}}_m \quad (16)$$

$$\begin{aligned}
 \rho((\tilde{\mathbf{u}}_m \cdot \nabla)k + (\mathbf{u} \cdot \nabla)\tilde{k}_m) &= \left(\nabla \frac{\tilde{\mu}_m}{\sigma_k} \right) \cdot (\nabla k) + \frac{\tilde{\mu}_m}{\sigma_k} \Delta k + \left(\nabla \frac{\mu_t}{\sigma_k} \right) \cdot (\nabla \tilde{k}_m) \\
 &+ \frac{\mu_t}{\sigma_k} \Delta \tilde{k}_m + \rho \tilde{P}_{km} - \rho \tilde{\varepsilon}_m + q_{km} \quad (17)
 \end{aligned}$$

$$\begin{aligned} \rho((\tilde{\mathbf{u}}_m \cdot \nabla)\varepsilon + (\mathbf{u} \cdot \nabla)\tilde{\varepsilon}_m) &= \left(\nabla \frac{\tilde{\mu}_m}{\sigma_\varepsilon}\right) \cdot (\nabla \varepsilon) + \frac{\tilde{\mu}_m}{\sigma_\varepsilon} \Delta \varepsilon + \left(\nabla \frac{\mu_t}{\sigma_\varepsilon}\right) \cdot (\nabla \tilde{\varepsilon}_m) + \frac{\mu_t}{\sigma_k} \Delta \tilde{\varepsilon}_m \\ &+ \rho C_{\varepsilon 1} \frac{\varepsilon}{k} \tilde{P}_{km} + \frac{\rho P_k C_{\varepsilon 1} - 2\rho \varepsilon}{k} \tilde{\varepsilon}_m - \frac{\rho P_k C_{\varepsilon 1} \varepsilon - \rho \varepsilon^2}{k^2} \tilde{k}_m + q_{\varepsilon m} \end{aligned} \quad (18)$$

$$\tilde{\mu}_m - \rho C_\mu \frac{2k}{\varepsilon} \tilde{k}_m + \rho C_\mu \frac{k^2}{\varepsilon^2} \tilde{\varepsilon}_m = q_{\mu m} \quad (19)$$

where the derivative production may be expressed using the following equations:

$$\rho \tilde{P}_{km} = \tilde{\mu}_m S^2 + 2\mu_t \tilde{S}^2, \quad \tilde{S} \equiv \sqrt{2s_{ij}\tilde{s}_{ijm}}, \quad \tilde{s}_{ij} = \frac{1}{2} \left(\frac{\partial \tilde{u}_{im}}{\partial x_j} + \frac{\partial \tilde{u}_{jm}}{\partial x_i} \right) \quad (20)$$

and q_{km} , $q_{\varepsilon m}$ and $q_{\mu m}$ are terms of the right-hand side and their relationship to each parameter is described with the following equations:

- for the $C_{\varepsilon 1}$ parameter:

$$q_{\varepsilon 1} = P_k \frac{\varepsilon}{k} \quad (21)$$

- for the $C_{\varepsilon 2}$ parameter:

$$q_{\varepsilon 2} = -\rho \frac{\varepsilon^2}{k} \quad (22)$$

- for the C_μ parameter:

$$q_{\mu 3} = \rho \frac{k^2}{\varepsilon} \quad (23)$$

- for the σ_k parameter:

$$q_{k4} = - \left(\nabla \frac{\mu_t}{\sigma_k^2} \right) \cdot (\nabla k) - \frac{\mu_t}{\sigma_k^2} \Delta k \quad (24)$$

- for the σ_ε parameter:

$$q_{\varepsilon 5} = - \left(\nabla \frac{\mu_t}{\sigma_\varepsilon^2} \right) \cdot (\nabla \varepsilon) - \frac{\mu_t}{\sigma_\varepsilon^2} \Delta \varepsilon \quad (25)$$

The system of differential equations (15)–(19) needs to be supplemented with boundary conditions resulting from assuming the actual boundary condition types for the analysed flow. Thus, assuming for the main problem that the properties are constant at the edge means that the sensitivity coefficient equals zero ($\tilde{p}_m = 0$, $\tilde{u}_{1m} = 0$, $\tilde{u}_{2m} = 0$, $\tilde{k}_m = 0$, $\tilde{\varepsilon}_m = 0$ and $\tilde{\mu}_m = 0$) because the flow properties do not depend on the model parameters. Consequently, if we assume that at boundary conditions corresponding derivatives of flow properties s with respect to the coordinates x_i are zero:

$$\frac{\partial s}{\partial x_i} = 0 \quad (26)$$

then the derivatives of the sensitivity coefficients \tilde{s}_m in relation to these coordinates x_i are also zero:

$$\frac{\partial^2 s}{\partial x_i \partial C_m} = \frac{\partial \tilde{s}}{\partial x_i} = 0 \quad (27)$$

Additionally, for the areas near the wall, Equations (15)–(19) of the system should be modified by considering the boundary layer model, which was used to determine the flow properties.

In order to solve the system of Equations (15)–(19), it would be better to solve an earlier main problem of the flow with the nominal parameter values (described by Equations (1)–(5)), and only then can the problem of sensitivity analysis be solved with similar numerical methods and the suitable boundary conditions. Of course, the sets of Equations (1)–(5) and (15)–(19) can be solved simultaneously, but it causes an increase in the computer memory amount needed and quadruple growth of the calculation time in comparison with the set of five differential equations.

The equations presented in this paper are prepared by the author (comp. Błazik-Borowa [20]) irrespective of Colin *et al.* [21], where sensitivity analysis for flows is considered as well. The differences between their researches and obtained solutions are as follows:

- Colin *et al.* [21] performed an analysis for temperature flows and the author of this paper for the flow without temperature, but for high Reynolds number;
- Colin *et al.* [21] determined the sensitivity coefficients for the logarithmic form of equations for turbulence kinetic energy and dissipation rate;
- Colin *et al.* [21] applied the forward sensitivity analysis based on the finite element method whereas the author proposed two methods of obtaining the sensitivity coefficients: a finite difference approximation to the sensitivity coefficients and the forward sensitivity analysis based on the finite volume method.

The sensitivity analysis has many applications in the engineering practice. For example, in this paper the sensitivity analysis of the channel flow is made and on the basis of the results of this analysis the assessment of boundary layers with regard to the sensitivity to turbulence model parameters is performed. In other papers of the author [22–24] the sensitivity analysis has been used for the assessment of the sensitivity of the flow around a single and two square cylinders to the model parameters and the determination of the influence of the input flow properties on quality results. Colin *et al.* [21] proposed the application of the sensitivity analysis to identify key parameters for controlling the flow and to estimate the errors of the skin frictions and Stanton number for the heated backward facing step.

4. THE CHANNEL FLOW SENSITIVITY TO THE PARAMETERS OF THE k - ε METHOD

4.1. Results of the channel flow calculations

Further analyses will be made for the flow in a square pipe (channel). Results of tests for this problem have been described in detail in papers [25, 26]. Dimensions of the channel, the grid of the finite volume method and boundary conditions for this problem are presented in Figure 1. Flow properties at velocity inlet no. 1 are constant values of the components of velocity $u_0 = u_{01} = 6.7 \text{ m/s}$

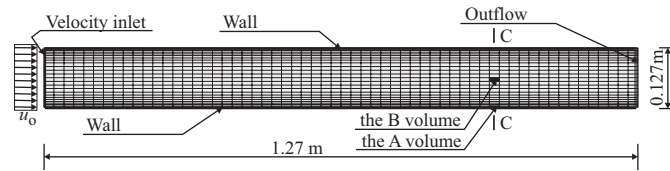


Figure 1. The model grid for the finite volume method with dimensions and boundary conditions for the channel flow.

and $u_{02}=0\text{ m/s}$, the turbulence intensity $I_u=4.4\%$ and the hydraulic diameter $D_h=0.127\text{ m}$, which gives the Reynolds number $Re=55\,000$. The model contains 1440 cells, 1525 nodes and 2964 edges. As nominal parameter values, the ones suggested as default by FLUENT, i.e. $C_{\epsilon 1}=1.44$, $C_{\epsilon 2}=1.92$, $C_\mu=0.09$, $\sigma_k=1.0$ and $\sigma_\epsilon=1.3$, have been assumed.

Following paper [25], Figure 2 presents the research results presented in the paper by Viegas *et al.* [26]. The graphs include measurement results in the channel and the calculation results in the C cross section at about $\frac{3}{4}$ length of the channel (comp. Figure 1) for three different models of boundary layers. In Figure 3 the differences between the measurement and calculation results for the velocity and turbulence kinetic energy for three models of boundary layers are shown as well.

As it is seen in Figures 2(b) and (d) and 3, in the middle of the graphs, at $y=0$, a fairly good correspondence of calculations and tests was obtained, whereas in the boundary layer, the calculated turbulence kinetic energy is almost twice as large as the one obtained by the measurement. Kim [25] also gave the measured value of the pressure gradient along the wall that equals -1.4 Pa/m . From calculations with the first two models, i.e. using the boundary layer function, the gradient of -2.06 Pa/m was obtained, whereas the third model gave the gradient of -2.18 Pa/m . This means that the pressure gradient is, unfortunately, incorrectly determined.

4.2. The channel flow sensitivity analysis

In order to determine the sensitivity coefficients of six flow properties for five parameters for the standard $k-\epsilon$ turbulence model, the finite difference approach will be used. This method requires evaluation of increments of the model parameters ΔC_m for which sensitivity analysis is correct and therefore many calculations were made for different values of the model parameters to check the shape of flow property functions when changing these parameters. Figures 4–8 present graphs of flow properties variation depending on the model parameters at two points: near the wall, the volume A and in the middle of flow, the volume B, for the problem of Figure 1 with boundary layer model no. 1. The cells, in which the calculation results are analysed, are located at about $\frac{3}{4}$ length of the channel where the vertical profile is fully formed. In this case, the graphs around the nominal parameter values are almost linear, which means that the calculations made with the finite difference approximation at $\Delta C_{\epsilon 1}=\Delta C_{\epsilon 2}=\Delta\sigma_k=\Delta\sigma_\epsilon=0.1$, $\Delta C_\mu=0.01$ will give correct results in relation to the flow properties sensitivity.

Based on the sensitivity analysis, 30 fields of sensitivity coefficients are obtained for one problem. Examples of fields for the whole flow are presented in Figures 9–13. Relative extreme values are compared in Figures 14–16 and graphs of all sensitivity coefficients in the C cross section of the channel are presented in Figures 17–22.

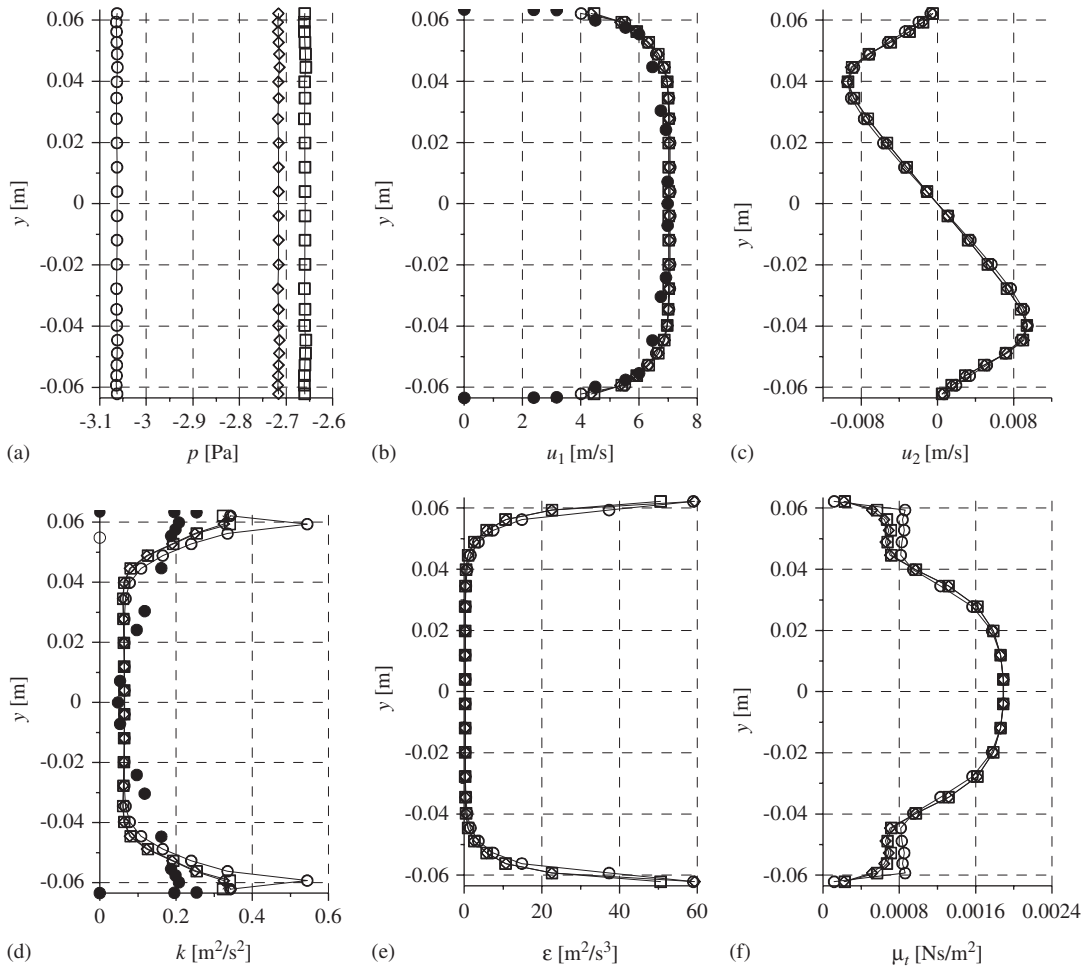


Figure 2. The calculation results of flow properties at the cross section of the channel at $u_{01}=6.7\text{ m/s}$, $Re=55000$ and parameters: $C_\mu=0.09$, $C_{\varepsilon 1}=1.44$, $C_{\varepsilon 2}=1.92$, $\sigma_k=1.0$ and $\sigma_\varepsilon=1.3$: (a) the pressure p ; (b) the velocity u_1 ; (c) the velocity u_2 ; (d) the turbulence kinetic energy k ; (e) the dissipation rate ε of turbulence kinetic energy; and (f) the turbulence dynamic viscosity μ_t . ●, research results based on paper [25]; calculation results for: ◇, model no. 1 for the boundary layer; □, model no. 2 for the boundary layer and ○, model no. 3 for the boundary layer.

The interpretation of the results of the sensitivity analysis is as follows: as the sensitivity coefficients are derivatives of properties with respect to the parameters, the negative values of coefficients mean that the flow properties are decreasing functions of the parameters and the positive values mean they are increasing functions. The sensitivity indicates the qualitative changes of the flow properties only. In the case of small changes in the parameter, it is possible to determine the approximate property value that will be obtained from the problem with new values of parameters. For example, $\tilde{k}_{C_\mu}=-2.767\text{ m}^2/\text{s}^2$ from the table in Figure 14 means that increasing the C_μ

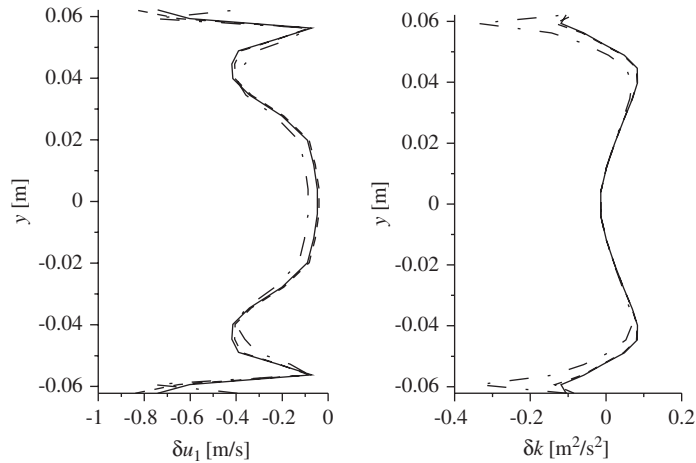


Figure 3. The differences between measurements and calculations for the velocity (δu_1) and the turbulence kinetic energy (δk) along the C cross section of the channel. —, model no. 1 for the boundary layer; - - - - model no. 2 for the boundary layer and - · - · - model no. 3 for the boundary layer.

parameter by 10%, i.e. changing it by 0.009, may result in a decrease in the turbulence kinetic energy by 0.0249 in the volume of the largest sensitivity. In practice, this means that within a small range around the nominal model parameter values the obtained results may be corrected so that they are closer to the measurement results, of course, if the first set of nominal parameter values is close to correct values. It can be assured with the determination of nominal parameter values from Equations (6)–(11) and the comparison of obtained values of parameters to the ones used by other researchers.

Moreover the particular parameters can have a quite different influence on the numerical solution. Therefore, it is worth checking the total influence of all model parameters on calculation results and it can be calculated from the following equations:

$$\Delta p = \tilde{p}_{C_{\varepsilon 1}} dC_{\varepsilon 1} + \tilde{p}_{C_{\varepsilon 2}} dC_{\varepsilon 2} + \tilde{p}_{C_{\mu}} dC_{\mu} + \tilde{p}_{\sigma_k} d\sigma_k + \tilde{p}_{\sigma_{\varepsilon}} d\sigma_{\varepsilon} \quad (28)$$

$$\Delta u_1 = \tilde{u}_{1C_{\varepsilon 1}} dC_{\varepsilon 1} + \tilde{u}_{1C_{\varepsilon 2}} dC_{\varepsilon 2} + \tilde{u}_{1C_{\mu}} dC_{\mu} + \tilde{u}_{1\sigma_k} d\sigma_k + \tilde{u}_{1\sigma_{\varepsilon}} d\sigma_{\varepsilon} \quad (29)$$

$$\Delta u_2 = \tilde{u}_{2C_{\varepsilon 1}} dC_{\varepsilon 1} + \tilde{u}_{2C_{\varepsilon 2}} dC_{\varepsilon 2} + \tilde{u}_{2C_{\mu}} dC_{\mu} + \tilde{u}_{2\sigma_k} d\sigma_k + \tilde{u}_{2\sigma_{\varepsilon}} d\sigma_{\varepsilon} \quad (30)$$

$$\Delta k = \tilde{k}_{C_{\varepsilon 1}} dC_{\varepsilon 1} + \tilde{k}_{C_{\varepsilon 2}} dC_{\varepsilon 2} + \tilde{k}_{C_{\mu}} dC_{\mu} + \tilde{k}_{\sigma_k} d\sigma_k + \tilde{k}_{\sigma_{\varepsilon}} d\sigma_{\varepsilon} \quad (31)$$

$$\Delta \varepsilon = \tilde{\varepsilon}_{C_{\varepsilon 1}} dC_{\varepsilon 1} + \tilde{\varepsilon}_{C_{\varepsilon 2}} dC_{\varepsilon 2} + \tilde{\varepsilon}_{C_{\mu}} dC_{\mu} + \tilde{\varepsilon}_{\sigma_k} d\sigma_k + \tilde{\varepsilon}_{\sigma_{\varepsilon}} d\sigma_{\varepsilon} \quad (32)$$

$$\Delta \mu_t = \tilde{\mu}_{C_{\varepsilon 1}} dC_{\varepsilon 1} + \tilde{\mu}_{C_{\varepsilon 2}} dC_{\varepsilon 2} + \tilde{\mu}_{C_{\mu}} dC_{\mu} + \tilde{\mu}_{\sigma_k} d\sigma_k + \tilde{\mu}_{\sigma_{\varepsilon}} d\sigma_{\varepsilon} \quad (33)$$

where $dC_{\varepsilon 1}$, $dC_{\varepsilon 2}$, dC_{μ} , $d\sigma_k$, $d\sigma_{\varepsilon}$ are analysed increments of the parameters. The results, presented in Figure 2, are calculated for $dC_{\varepsilon 1} = 0.05C_{\varepsilon 1}$, $dC_{\varepsilon 2} = 0.05C_{\varepsilon 2}$, $dC_{\mu} = 0.05C_{\mu}$, $d\sigma_k = 0.05\sigma_k$ and $d\sigma_{\varepsilon} = 0.05\sigma_{\varepsilon}$. The increments of flow properties, which are determined based on the above equations, are shown in Figure 23.

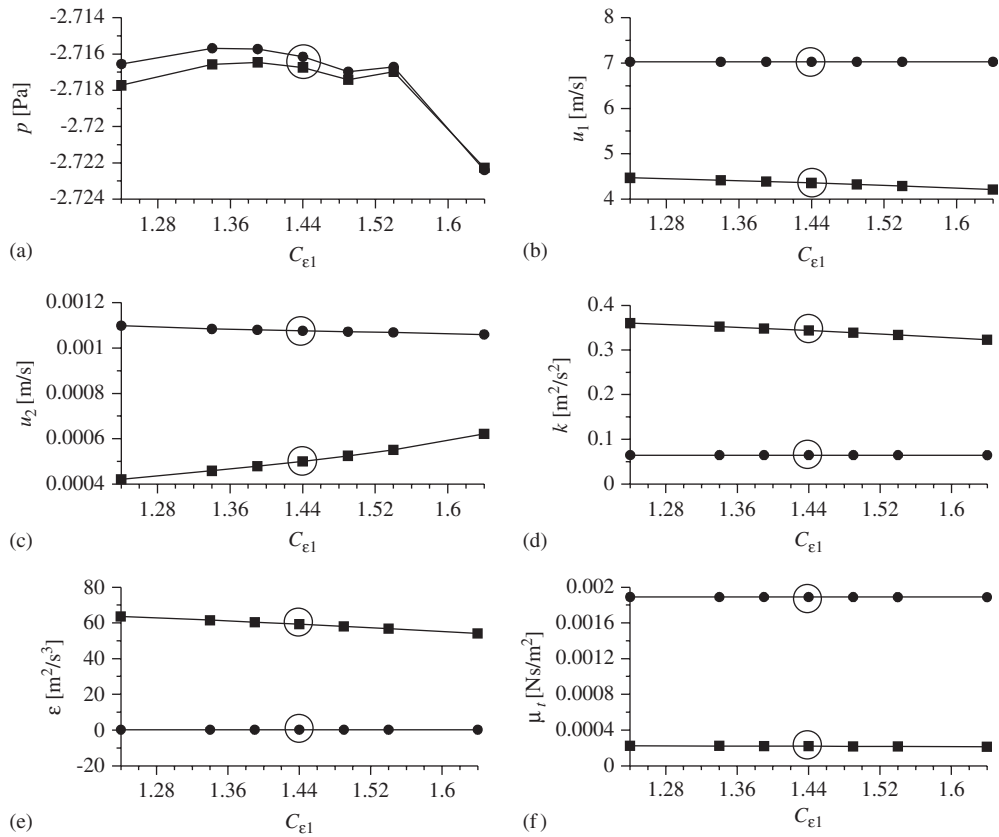


Figure 4. The graphs of the flow properties in the function of the $C_{\epsilon 1}$ parameter: (a) the pressure; (b) the component of velocity along the model; (c) the component of velocity in the direction perpendicular to the length of the model; (d) the turbulence kinetic energy; (e) the turbulence dissipation rate; and (f) the turbulence dynamic viscosity. ■, results of the *A* volume and □, results of the *B* volume.

It should be noted that the change of model parameters in the main problem causes the change of sensitivity coefficients. In Figure 24 the graphs of the sensitivity coefficients as functions of parameters are shown. As it may be seen the changes of values of all parameters caused the significant changes of the sensitivity coefficients. Hence next revision of numerical results with regard to parameters has to be made with new values of sensitivity coefficients. Revisions for small increments of the parameters can be made a few times to obtain the best results. It seems that such calibration of parameters in order to improve the calculation results is possible, but it is a very broad problem and can be the subject of another paper.

Figures 9–13 present selected examples of sensitivity coefficient fields. Forms of fields for individual sensitivity coefficients are not, practically, different for different models of the boundary layer. On the other hand, there are significant differences between coefficients of individual properties. The velocity sensitivity value increases along the channel, sensitivity of the turbulence kinetic energy assumes significant values in the area of profile forming, i.e. in the first part of the channel,

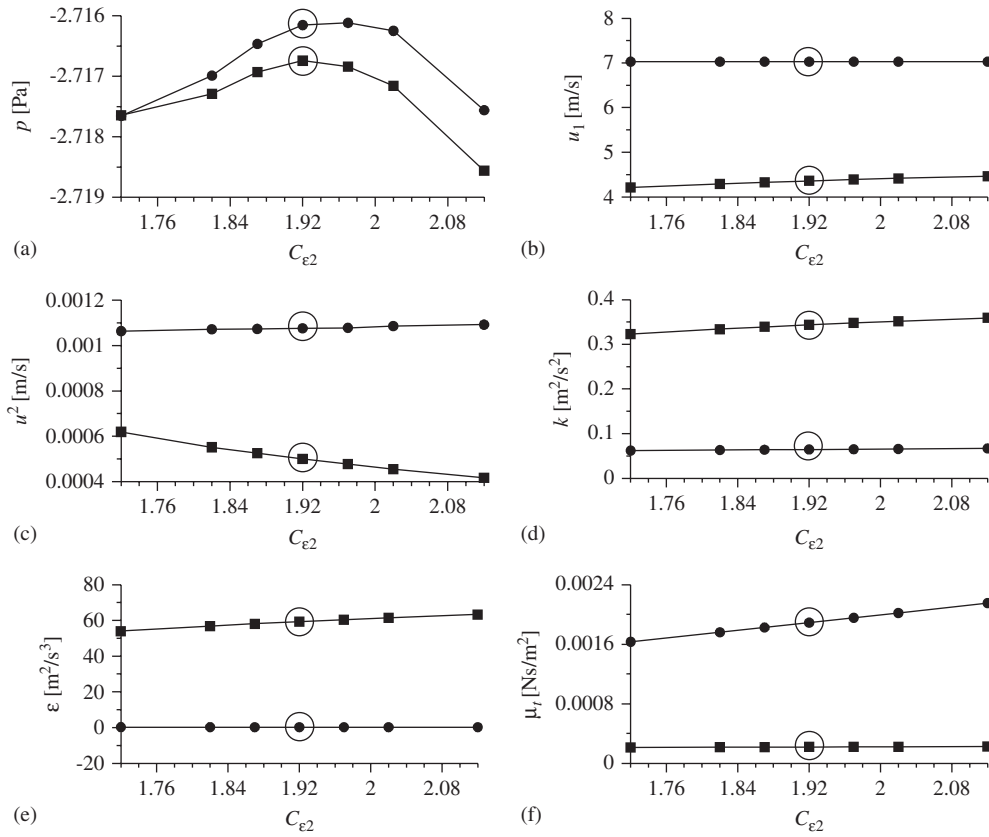


Figure 5. The graphs of the flow properties in the function of the $C_{\epsilon 2}$ parameter: (a) the pressure; (b) the component of velocity along the model; (c) the component of velocity in the direction perpendicular to the length of the model; (d) the turbulence kinetic energy; (e) the turbulence dissipation rate; and (f) the turbulence dynamic viscosity. ■, results of the *A* volume and □, results of the *B* volume.

and then it decreases. The dissipation is the most sensitive to the model parameters at the channel inlet.

Within the initial area where the velocity profile shape changes, all flow properties are very sensitive to the model parameters. Unfortunately, the areas of extreme values are usually small, which means that they are invisible on the contour maps. Figures 14–16 present relative and absolute extreme values that mostly correspond to the volumes near the wall of the first part of the channel. The figures present the relative values with regard to the value at the inflow and are described in the following manner:

- relative sensitivity coefficients of the p pressure:

$$\tilde{p}_m = \frac{\frac{\partial p}{\partial C_m}}{0.5\rho u_0^2} = \frac{\tilde{p}_m}{0.5\rho u_0^2} \tag{34}$$

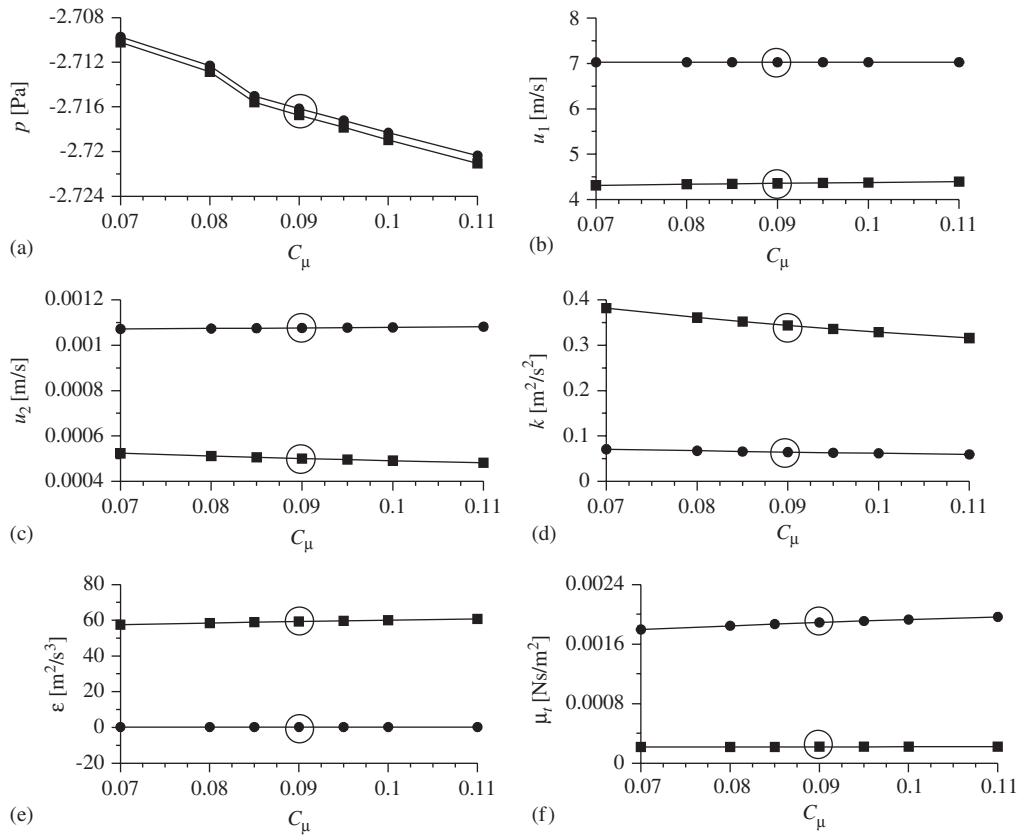


Figure 6. The graphs of the flow properties in the function of the C_μ parameter: (a) the pressure; (b) the component of velocity along the model; (c) the component of velocity in the direction perpendicular to the length of the model; (d) the turbulence kinetic energy; (e) the turbulence dissipation rate; and (f) the turbulence dynamic viscosity. ■, results of the A volume and □, results of the B volume.

- relative sensitivity coefficients of the u_1 velocity component:

$$\tilde{u}_{1m} = \frac{\frac{\partial u_1}{\partial C_m}}{u_0} = \frac{\tilde{u}_{1m}}{u_0} \quad (35)$$

- relative sensitivity coefficients of the u_2 velocity component:

$$\tilde{u}_{2m} = \frac{\frac{\partial u_2}{\partial C_m}}{u_0} = \frac{\tilde{u}_{2m}}{u_0} \quad (36)$$

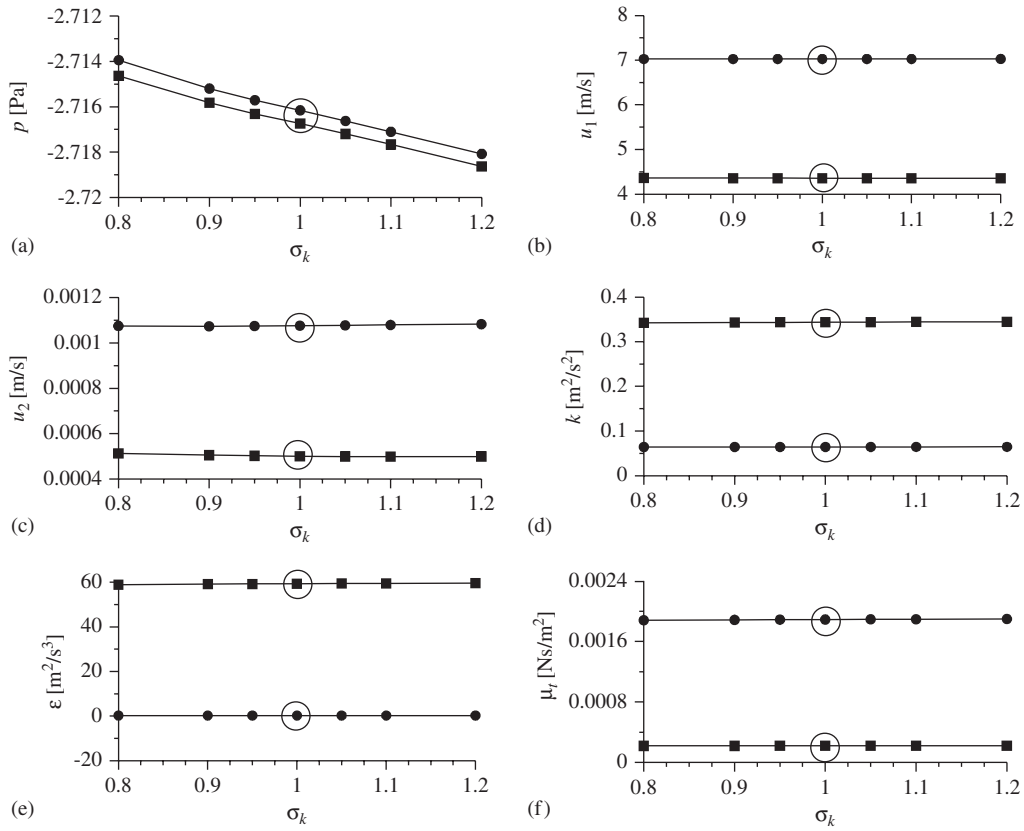


Figure 7. The graphs of the flow properties in the function of the σ_k parameter: (a) the pressure; (b) the component of velocity along the model; (c) the component of velocity in the direction perpendicular to the length of the model; (d) the turbulence kinetic energy; (e) the turbulence dissipation rate; and (f) the turbulence dynamic viscosity. ■, results of the A volume and □, results of the B volume.

- relative sensitivity coefficients of the k turbulence kinetic energy:

$$\tilde{k}_m = \frac{\frac{\partial k}{\partial C_m}}{k_0} = \frac{\tilde{k}_m}{k_0} \tag{37}$$

- relative sensitivity coefficients of the ε dissipation rate of turbulence kinetic energy:

$$\tilde{\varepsilon}_m = \frac{\frac{\partial \varepsilon}{\partial C_m}}{\varepsilon_0} = \frac{\tilde{\varepsilon}_m}{\varepsilon_0} \tag{38}$$

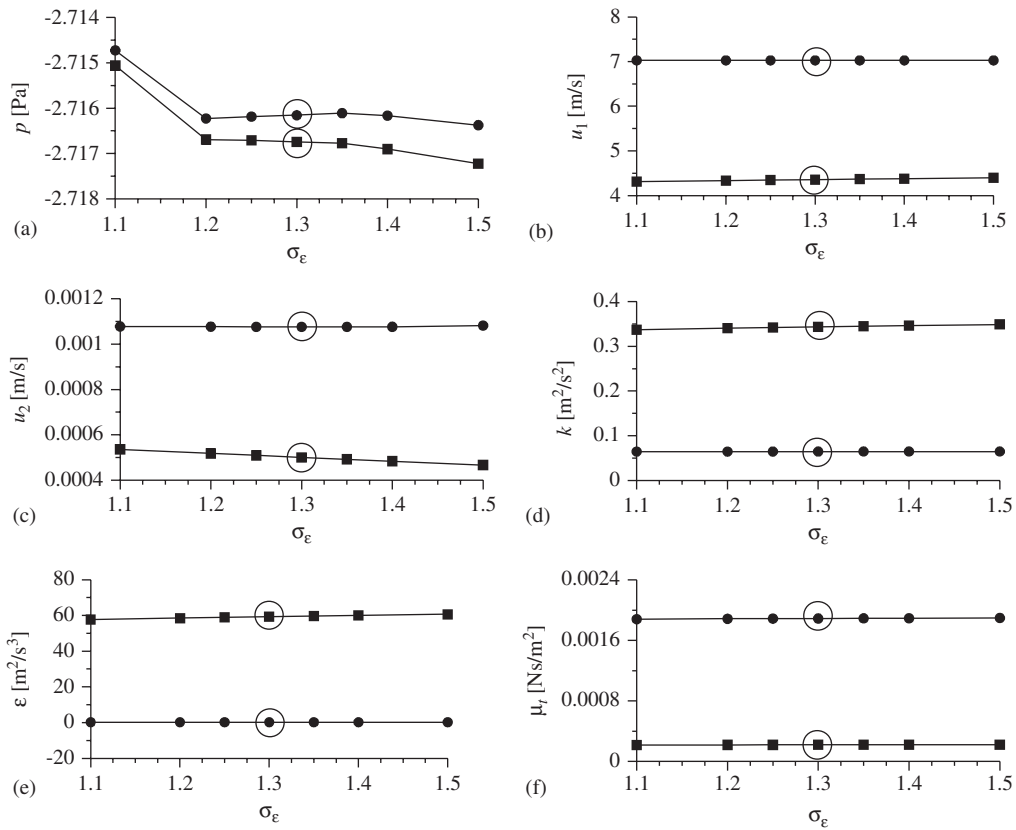


Figure 8. The graphs of the flow properties in the function of the σ_ϵ parameter: (a) the pressure; (b) the component of velocity along the model; (c) the component of velocity in the direction perpendicular to the length of the model; (d) the turbulence kinetic energy; (e) the turbulence dissipation rate; and (f) the turbulence dynamic viscosity. ■, results of the A volume and □, results of the B volume.

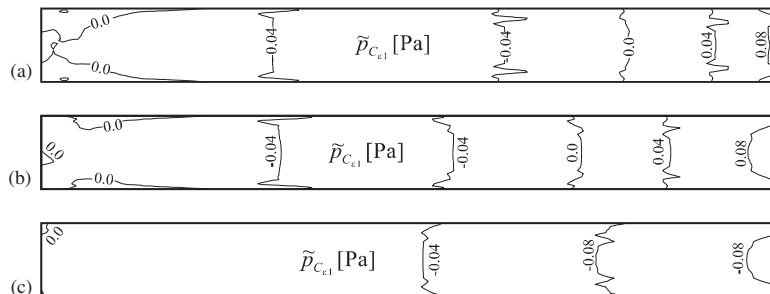


Figure 9. The fields of the pressure sensitivity to the C_{e1} parameter at $u_0=6.7$ m/s, $Re=55000$ and the parameters $C_\mu=0.09$, $C_{\epsilon 1}=1.44$, $C_{\epsilon 2}=1.92$, $\sigma_k=1.0$ and $\sigma_\epsilon=1.3$ for (a) model no. 1; (b) model no. 2; and (c) model no. 3.

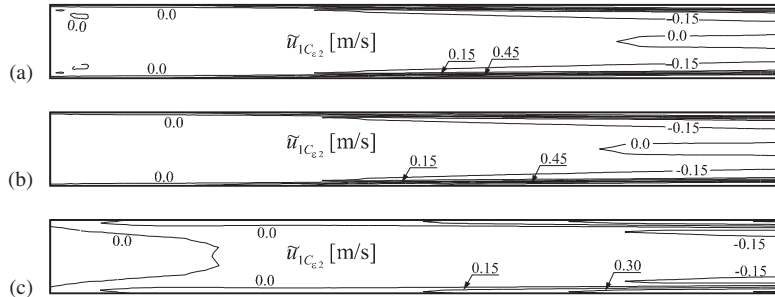


Figure 10. The fields of the velocity sensitivity to the $C_{\epsilon 2}$ parameter at $u_0=6.7$ m/s, $Re=55000$ and the parameters $C_\mu=0.09$, $C_{\epsilon 1}=1.44$, $C_{\epsilon 2}=1.92$, $\sigma_k=1.0$ and $\sigma_\epsilon=1.3$ for (a) model no. 1; (b) model no. 2; and (c) model no. 3.

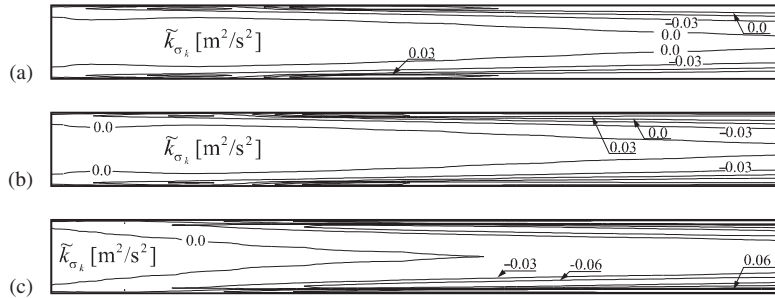


Figure 11. The fields of the sensitivity of a turbulence kinetic energy to the σ_k parameter at $u_0=6.7$ m/s, $Re=55000$ and the parameters $C_\mu=0.09$, $C_{\epsilon 1}=1.44$, $C_{\epsilon 2}=1.92$, $\sigma_k=1.0$ and $\sigma_\epsilon=1.3$ for (a) model no. 1; (b) model no. 2; and (c) model no. 3.

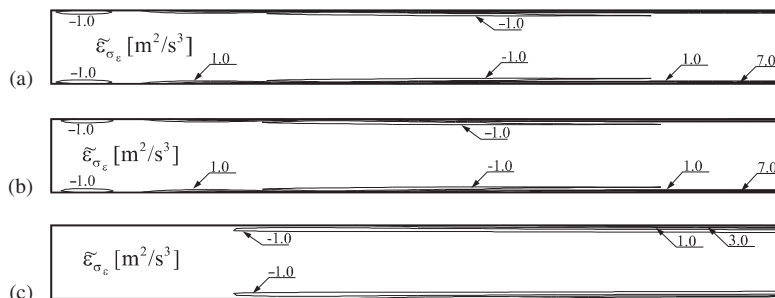


Figure 12. The fields of the sensitivity of a dissipation rate to the σ_ϵ parameter at $u_0=6.7$ m/s, $Re=55000$ and the parameters $C_\mu=0.09$, $C_{\epsilon 1}=1.44$, $C_{\epsilon 2}=1.92$, $\sigma_k=1.0$ and $\sigma_\epsilon=1.3$ for (a) model no. 1; (b) model no. 2; and (c) model no. 3.

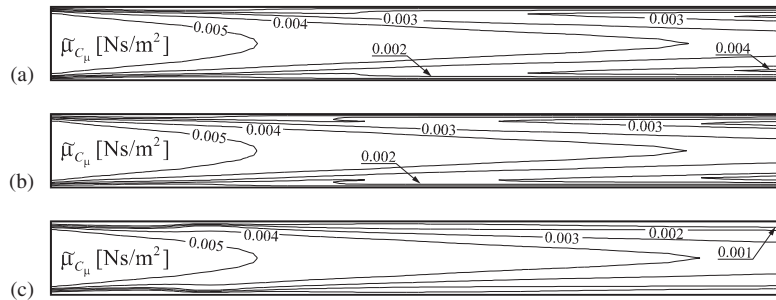


Figure 13. The fields of the sensitivity of a turbulence dynamic viscosity to the C_μ parameter at $u_0 = 6.7$ m/s, $Re = 55000$ and the parameters $C_\mu = 0.09$, $C_{\varepsilon 1} = 1.44$, $C_{\varepsilon 2} = 1.92$, $\sigma_k = 1.0$ and $\sigma_\varepsilon = 1.3$ for (a) model no. 1; (b) model no. 2; and (c) model no. 3.

- relative sensitivity coefficients of the μ_t turbulence dynamic viscosity:

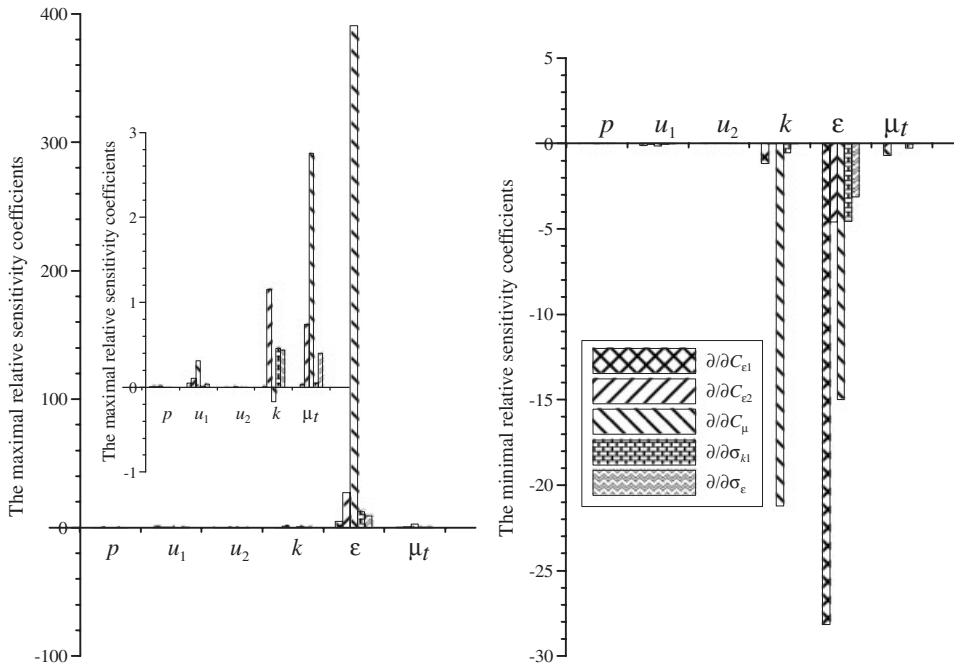
$$\tilde{\mu}_m = \frac{\partial \mu_t}{\partial C_m} = \frac{\tilde{\mu}_m}{\mu_{t0}} \quad (39)$$

where properties at the inflow are the velocity $u_0 = 6.7$ m/s, the turbulence kinetic energy $k_0 = 0.13036 \text{ m}^2/\text{s}^2$, the dissipation of turbulence kinetic energy $\varepsilon_0 = 0.91537 \text{ m}^2/\text{s}^3$ and the turbulence dynamic viscosity $\mu_{t0} = 0.002047 \text{ Ns/m}^2$.

In the graphs of Figures 14–16 the subsequent groups of data corresponding to the relative sensitivity coefficients of the properties are noted on the vertical axis. The descriptions of sensitivity coefficients as derivatives in relation to individual parameters are included in the keys to the figures. The comparison of the sensitivity value to the inflow value allows for comparing all sensitiveness of flow properties. In the tables of sensitivity coefficients, the largest values of sensitivity are shown in bold. The tables and graphs in the Figures 14–16 indicate that the most sensitive flow property to the model parameters is dissipation rate, followed by turbulence dynamic viscosity and turbulence kinetic energy with significantly smaller values of sensitivity. The flow properties depend, to the greatest extent, on the value of the C_μ parameter. The sensitivity to the parameters $C_{\varepsilon 1}$ and $C_{\varepsilon 2}$ is significantly smaller, but it should be noted that these parameters are also significantly bigger than the C_μ parameter. It means that the changes of parameters remaining in the same ranges (for example, 10%) cause similar changes of the flow properties. The parameters σ_k and σ_ε that are responsible for diffusion do not significantly affect the flow properties. The above conclusions are largely applicable to all calculations made, regardless of the boundary layer model.

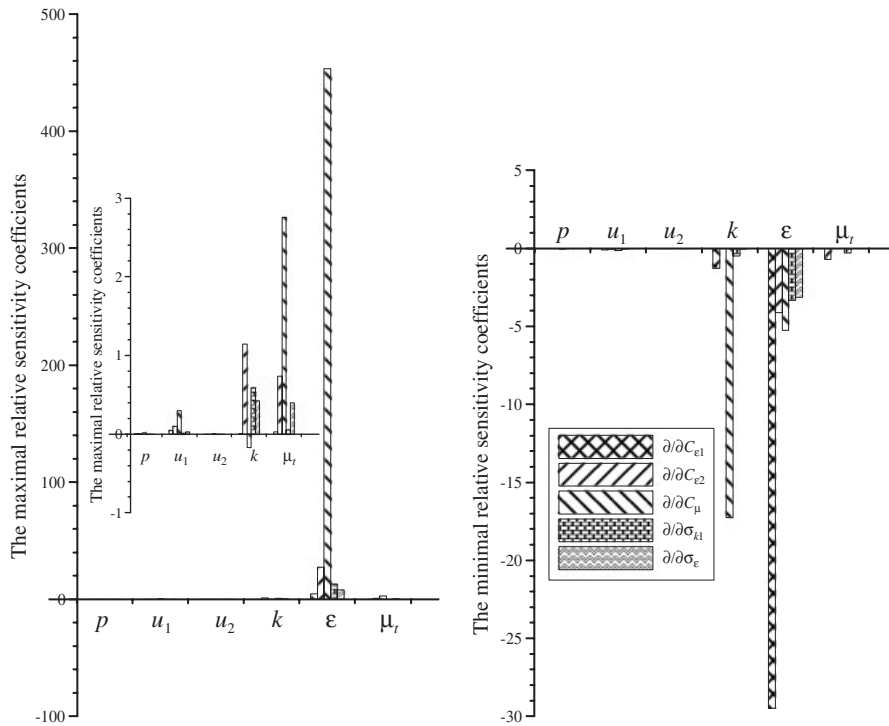
Figures 9–13 present only examples of the sensitivity coefficients distribution. Changes in all sensitivity coefficients in the channel cross section are presented in Figures 17–22. These results apply to the C cross section of the channel, i.e. from the cross section for which the graphs of Figure 2 were made. The analysed flow is the symmetrical problem with regard to the axis along the channel. The graphs of coefficients in Figures 17–22 show that the sensitivity analysis of the main problem is also a symmetrical exercise.

Moreover Figures 16–21 indicate that the results obtained in the middle part of the cross section for $y \in (-0.03 \text{ m}; 0.03 \text{ m})$ are independent of the parameters. This conclusion does not apply to pressure, as the sensitivity of this property is almost constant throughout the whole cross section,



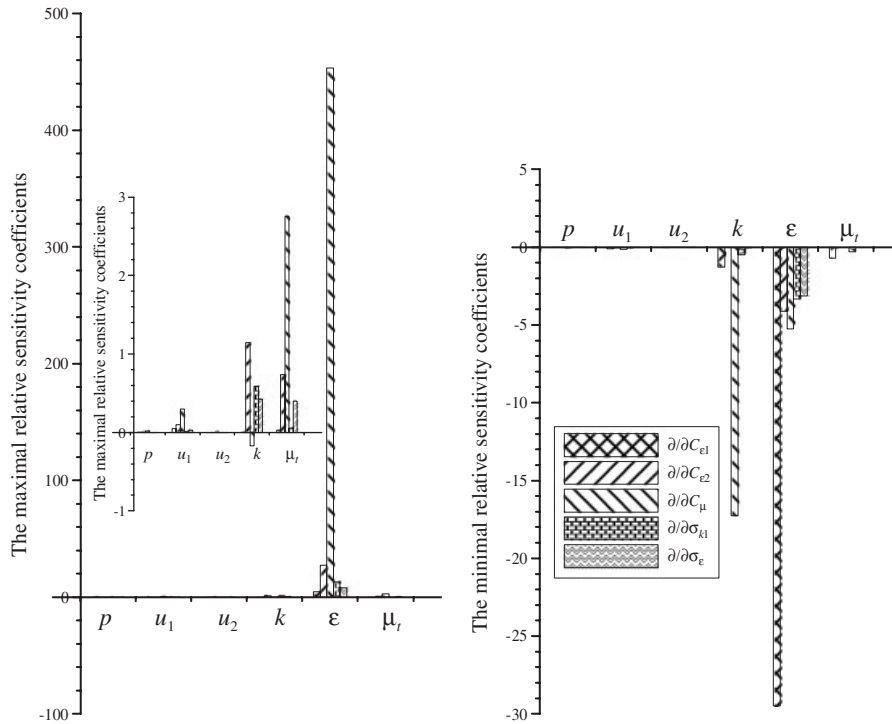
	$C_{\epsilon 1}$		$C_{\epsilon 2}$		C_{μ}		σ_k		σ_{ϵ}	
	min	max	min	max	min	max	min	max	min	max
\tilde{p}_m [Pa]	-0.0694	0.0890	-0.0955	0.0535	-0.5972	0.3615	-0.0516	0.0115	-0.0322	0.0212
\tilde{p}_m	-0.0025	0.0032	-0.0035	0.0019	-0.0217	0.0131	-0.0019	0.0004	-0.0012	0.0008
\tilde{u}_{1m} [m/s]	-0.7048	0.3187	-0.3092	0.6892	-0.9545	2.0917	-0.2750	0.0782	-0.1261	0.2373
\tilde{u}_{1m}	-0.1052	0.0476	-0.0462	0.1029	-0.1425	0.3122	-0.0410	0.0117	-0.0188	0.0354
\tilde{u}_{2m} [m/s]	-0.0066	0.0066	-0.0062	0.0062	-0.0284	0.0284	-0.0038	0.0038	-0.0028	0.0028
\tilde{u}_{2m}	-0.0010	0.0010	-0.0009	0.0009	-0.0042	0.0042	-0.0006	0.0006	-0.0004	0.0004
\tilde{k}_m [m ² /s ²]	-0.1516	0.0003	-0.0026	0.1499	-2.7670	-0.0224	-0.0705	0.0593	-0.0041	0.0570
\tilde{k}_m	-1.1629	0.0020	-0.0203	1.1501	-21.2259	-0.1719	-0.5410	0.4553	-0.0313	0.4370
$\tilde{\epsilon}_m$ [m ² /s ³]	-25.7837	4.3392	-4.2104	25.0528	-13.7366	357.797	-4.1909	11.0918	-2.8607	8.1936
$\tilde{\epsilon}_m$	-28.1675	4.7404	-4.5997	27.3690	-15.0066	390.877	-4.5784	12.1172	-3.1252	8.9511
$\tilde{\mu}_m$ [Ns/m ²]	-0.0014	0.00005	0	0.0015	0.00001	0.0056	-0.0006	0.0001	0	0.0008
$\tilde{\mu}_m$	-0.7013	0.0264	0	0.7364	0.0054	2.7521	-0.2780	0.0509	-0.0005	0.3984

Figure 14. Extreme values of relative and absolute sensitivity coefficients for the channel flow, with the use of model no. 1 for the boundary layer.



	$C_{\epsilon 1}$		$C_{\epsilon 2}$		C_{μ}		σ_k		σ_{ϵ}	
	min	max	min	max	min	max	min	max	min	max
\tilde{p}_m [Pa]	-0.0596	0.1096	-0.1077	0.0431	-1.3584	0.4807	-0.0485	0.0095	-0.0142	0.0188
\tilde{p}'_m	-0.0022	0.0040	-0.0039	0.0016	-0.0494	0.0175	-0.0018	0.0003	-0.0005	0.0007
\tilde{u}_{1m} [m/s]	-0.6808	0.3164	-0.3033	0.6466	-1.0057	2.0067	-0.2358	0.0652	-0.1182	0.2150
\tilde{u}'_{1m}	-0.1016	0.0472	-0.0453	0.0965	-0.1501	0.2995	-0.0352	0.0097	-0.0176	0.0321
\tilde{u}_{2m} [m/s]	-0.0066	0.0066	-0.0061	0.0061	-0.0359	0.0359	-0.0033	0.0033	-0.0028	0.0028
\tilde{u}'_{2m}	-0.0010	0.0010	-0.0009	0.0009	-0.0054	0.0054	-0.0005	0.0005	-0.0004	0.0004
\tilde{k}_m [m ² /s ²]	-0.1653	0.0003	-0.0022	0.1494	-2.2480	-0.0224	-0.0637	0.0762	-0.0058	0.0552
\tilde{k}'_m	-1.2681	0.0024	-0.0167	1.1459	-17.2445	-0.1719	-0.4887	0.5843	-0.0448	0.4232
$\tilde{\epsilon}_m$ [m ² /s ³]	-26.9901	3.9766	-3.7687	25.2089	-4.8012	414.959	-3.0384	11.7467	-2.8781	7.1378
$\tilde{\epsilon}'_m$	-29.4855	4.3467	-4.1172	27.5396	-5.2450	453.3230	-3.3192	12.8328	-3.1442	7.7977
$\tilde{\mu}_m$ [Ns/m ²]	-0.0015	0.0001	0	0.0015	0.0002	0.0056	-0.0001	0.0001	0	0.0008
$\tilde{\mu}'_m$	-0.7120	0.0293	0	0.7377	0.0989	2.7521	-0.2819	0.0538	-0.0003	0.4017

Figure 15. Extreme values of relative and absolute sensitivity coefficients for the channel flow, with the use of model no. 2 for the boundary layer.



	$C_{\epsilon 1}$		$C_{\epsilon 2}$		C_{μ}		σ_k		σ_{ϵ}	
	min	max	min	max	min	max	min	max	min	max
\tilde{P}_m [Pa]	-0.1253	0	0	0.1701	-0.2408	0.9164	-0.0996	0.0035	-0.0014	0.1068
\bar{P}_m	-0.0046	0	0	0.0062	-0.0088	0.0333	-0.0036	0.0001	-0.00005	0.0039
\tilde{u}_{1m} [m/s]	-0.4261	0.1938	-0.2086	0.4624	-0.9241	1.3035	-0.1984	0.1128	-0.1281	0.2468
\bar{u}_{1m}	-0.0636	0.0289	-0.0311	0.0690	-0.1379	0.1946	-0.0296	0.0168	-0.0191	0.0368
\tilde{u}_{2m} [m/s]	-0.0051	0.0051	-0.0059	0.0059	-0.0203	0.0203	-0.0031	0.0031	-0.0034	0.0034
\bar{u}_{2m}	-0.0008	0.0008	-0.0009	0.0009	-0.0030	0.0030	-0.0005	0.0005	-0.0005	0.0005
\tilde{k}_m [m ² /s ²]	-0.1701	0.00005	-0.0005	0.1445	-2.8115	-0.0224	-0.0822	0.0977	-0.0067	0.0687
\bar{k}_m	-1.3051	0.0004	-0.0036	1.1087	-21.5672	-0.1719	-0.6304	0.7498	-0.0515	0.5271
$\tilde{\epsilon}_m$ [m ² /s ³]	-17.3124	2.0437	-2.5831	16.3485	-33.5094	364.213	-1.5758	9.1694	-1.8833	5.2133
$\bar{\epsilon}_m$	-18.9130	2.2326	-2.8219	17.8600	-36.6075	397.886	-1.7215	10.0171	-2.0575	5.6953
$\tilde{\mu}_m$ [Ns/m ²]	-0.0012	0	0	0.0015	-0.0003	0.0056	-0.0009	0.0002	-0.00002	0.0010
$\bar{\mu}_m$	-0.5628	0	0	0.7389	-0.1320	2.7521	-0.4304	0.1020	-0.0078	0.4936

Figure 16. Extreme values of relative and absolute sensitivity coefficients for the channel flow, with the use of model no. 3 for the boundary layer.

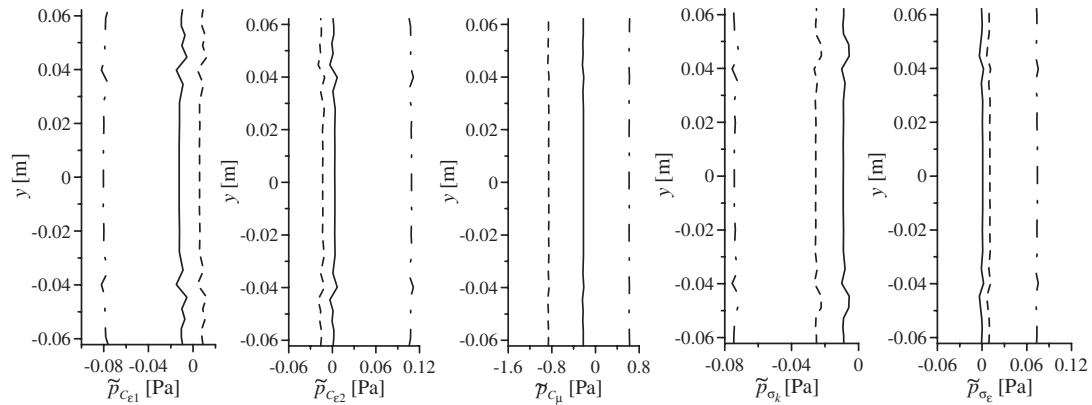


Figure 17. The sensitivity coefficients of pressure p along the channel cross section. —, model no. 1 for the boundary layer; ----, model no. 2 for the boundary layer and -·-·-, model no. 3 for the boundary layer.

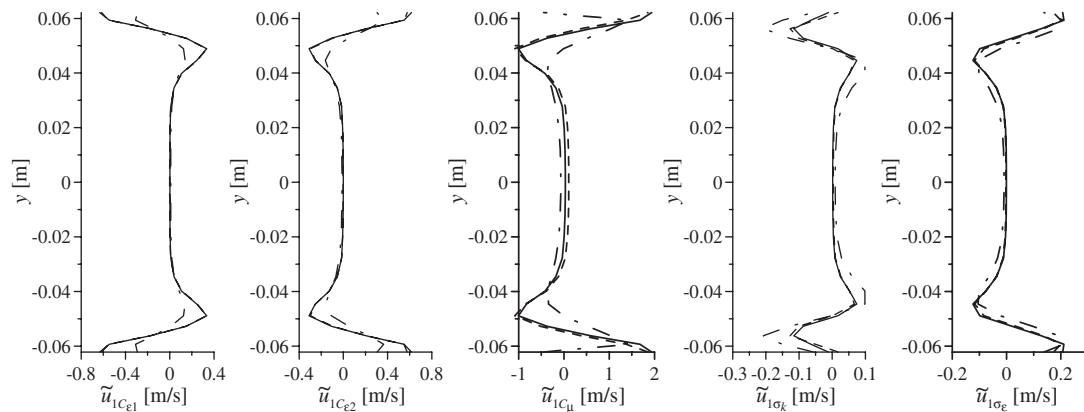


Figure 18. The sensitivity coefficients of the u_1 velocity component along the channel cross section. —, model no. 1 for the boundary layer; ----, model no. 2 for the boundary layer and -·-·-, model no. 3 for the boundary layer.

and to two sensitivity coefficients of the turbulence dynamic viscosity $\partial\mu_t/\partial C_{\epsilon 2}$ and $\partial\mu_t/\partial C_{\mu}$. The form of the graph $\partial\mu_t/\partial C_{\mu}$ arises from Equation (5), which describes the turbulence dynamic viscosity and includes the C_{μ} parameter, as well as from Equation (18). The former appears to show that if the energy and dissipation sensitivity coefficients are approximately zero, the sensitivity coefficients of the turbulence dynamic viscosity is close to zero as well, excluding the sensitivity in relation to the C_{μ} parameter.

A clear increase in sensitivity of most properties in the boundary layer may be detected in the graphs, whereas such coefficients as $\partial u_1/\partial C_{\epsilon 1}$, $\partial u_1/\partial C_{\epsilon 2}$, $\partial k/\partial C_{\mu}$ and all sensitivity coefficients of the dissipation rate assume their highest values near the wall, but there are also such coefficients that achieve their maximum in the area of the flow transition from the boundary

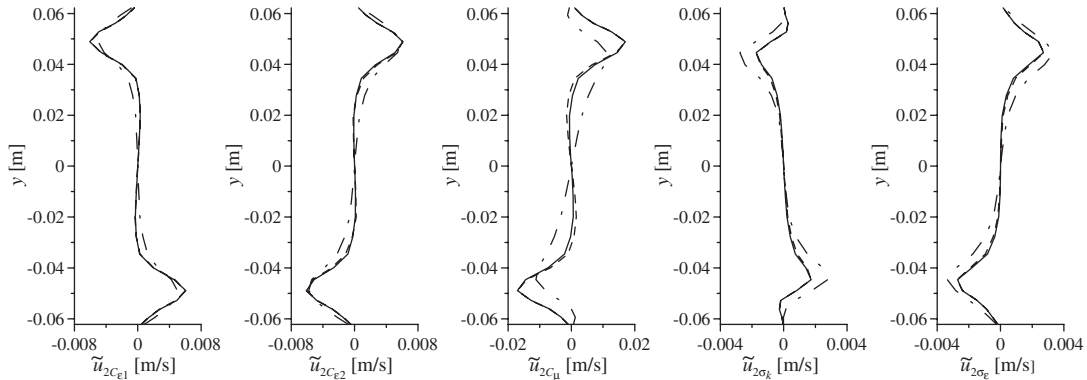


Figure 19. The sensitivity coefficients of the u_2 velocity component along the channel cross section. —, model no. 1 for the boundary layer; ----, model no. 2 for the boundary layer and -.-.- model no. 3 for the boundary layer.

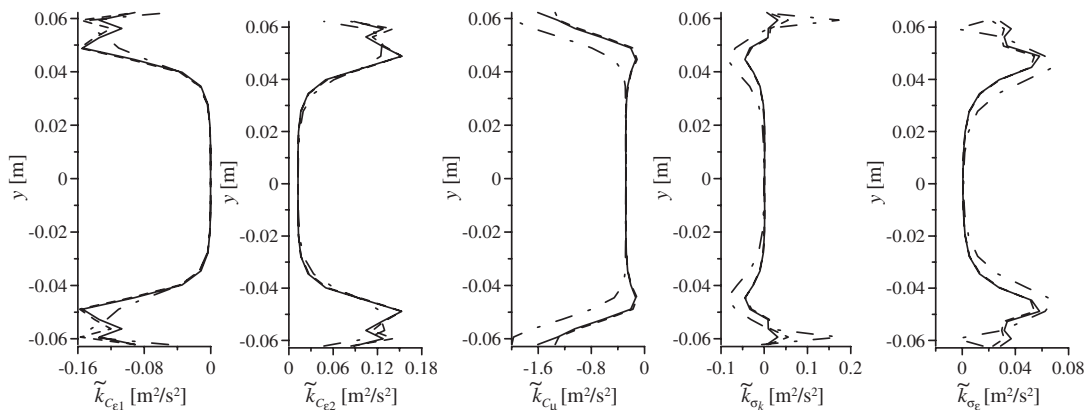


Figure 20. The sensitivity coefficients of the k turbulence kinetic energy along the channel cross section. —, model no. 1 for the boundary layer; ----, model no. 2 for the boundary layer; -.-.- model no. 3 for the boundary layer.

layer to the free stream. The latter coefficients include, but are not limited to, the following: $\partial k / \partial \sigma_k$, $\partial k / \partial \sigma_\epsilon$, $\partial \mu_t / \partial C_{\epsilon 1}$, $\partial \mu_t / \partial \sigma_k$, $\partial \mu_t / \partial \sigma_\epsilon$.

When comparing the results of calculations and measurements shown in Figures 2 and 3 to sensitivity analysis results from Figures 17–22 and 23, correlation between the areas of incorrect results and the graph areas of high sensitivity values is observable. The largest discrepancies between the calculations and measurements for the u_1 velocity are visible at $y \approx \pm 0.04$ and ± 0.06 m. This corresponds to the area where velocity sensitivity coefficients assume significant values, even up to 50% of their maximums, present at the wall. Moreover, a clear connection between the error in determining the turbulence kinetic energy and the turbulence kinetic energy sensitivity to the parameters is also observable (comp. Figures 3 and 20). It probably comes from the fact that the regions of significant sensitivities correspond to places with high gradients of flow

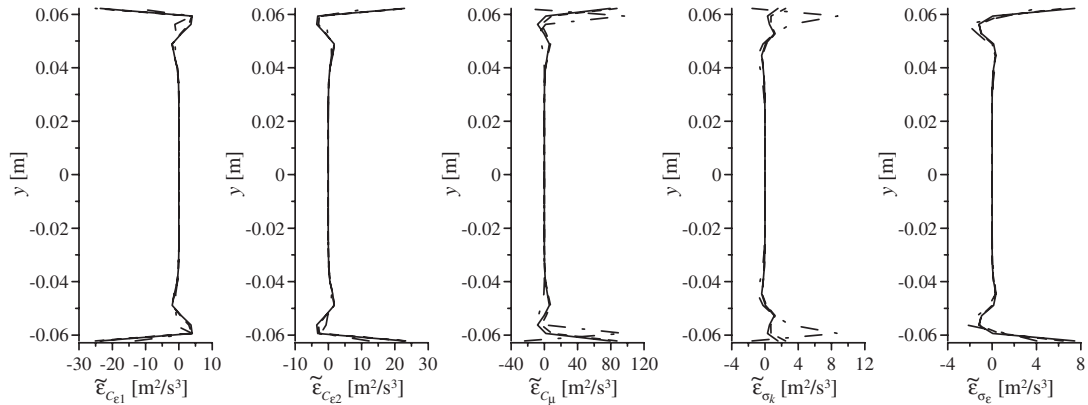


Figure 21. The sensitivity coefficients of the ε dissipation of turbulence kinetic energy along the channel cross section. —, model no. 1 for the boundary layer; ----, model no. 2 for the boundary layer and - · - · -, model no. 3 for the boundary layer.

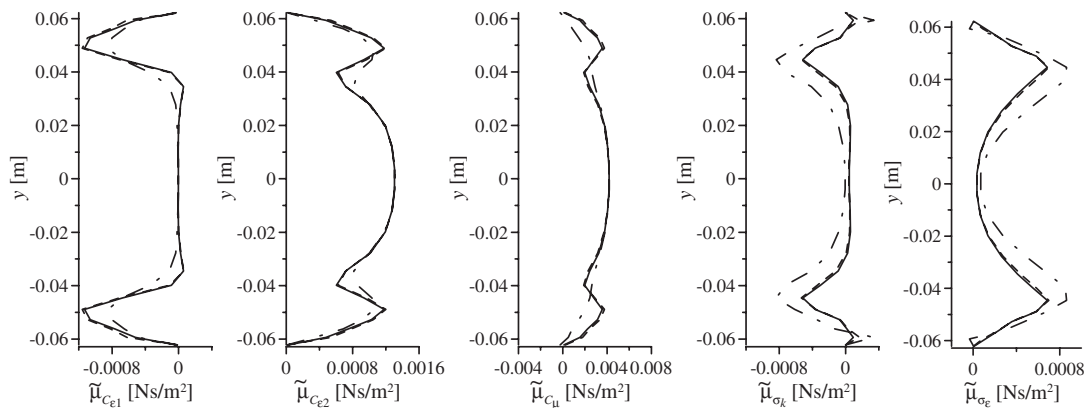


Figure 22. The sensitivity coefficients of the μ_t turbulence dynamic viscosity along the channel cross section C . —, model no. 1 for the boundary layer; ----, model no. 2 for the boundary layer and - · - · -, model no. 3 for the boundary layer.

properties. The model parameters are multipliers of the terms of Equations (1)–(5), which usually contain derivatives of flow properties with regard to coordinates. The high values of the terms cause the parameter from this term to significantly influence the results and the parameters from the small terms that have a smaller influence on them. Hence the high sensitivity can indicate significant errors of calculations that can be caused by both the wrong assumption of model parameters and the numerical errors that always exist for high gradients of approximated properties. Therefore the results of sensitivity analysis can be applied by the user of the CFD program to find the places where significant errors can be expected. For example, the dissipation rate is the most sensitive at the corners of the square and probably the values of this flow property are evaluated with big errors here.

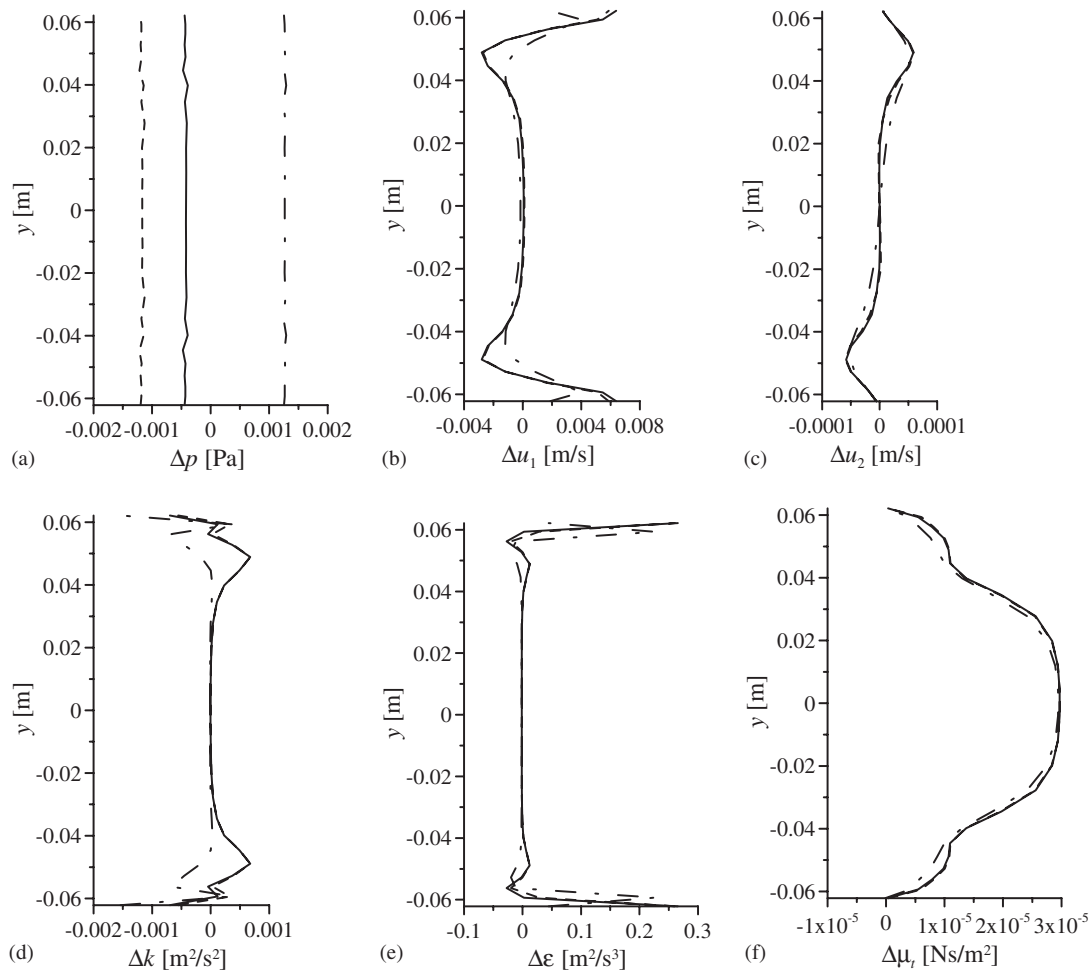


Figure 23. The altogether influence of model parameters on flow properties (Δp for pressure, Δu_1 for the u_1 velocity, Δu_2 for the u_2 velocity, Δk for the turbulence kinetic energy, $\Delta \varepsilon$ for the dissipation and $\Delta \mu_t$ for the turbulence dynamic viscosity) at the increase in parameters by 5%. —, model no. 1 for the boundary layer; ----, model no. 2 for the boundary layer and -·-·-, model no. 3 for the boundary layer.

However, the conclusion that says that the quality of solution is worst for highest sensitivity is not right for the problems with different FVM meshes and different methods of description of flow properties, which can cause the change of their derivatives in a space. For example, if because of too sparse mesh, the curvature of graphs of the flow properties decreases, we obtain the decrease in coefficients sensitivity as the result. In this case, the smaller sensitivity does not mean the better solution. The problem of the correlation between the quality solution and results of sensitivity analysis is very wide and it can be the subject of an other paper. This problem is initially described in the author's paper [24] and it will be developed in later researches.

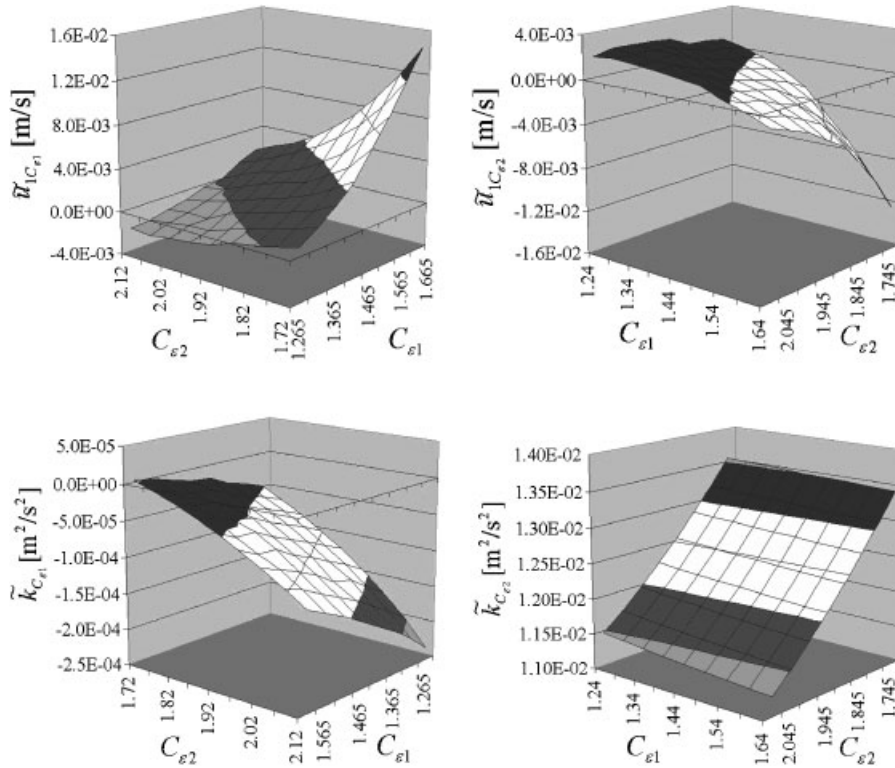


Figure 24. The graphs of exemplary sensitivity coefficients as functions of parameters $C_{\epsilon 1}$ and $C_{\epsilon 2}$ at the B volume.

4.3. The comparison of boundary layer models

The calculations were made with the use of three different boundary layer models described in Section 2.2. The calculation results do not differ much (Figure 2). The differences are larger in the graphs of sensitivity coefficients (Figures 9–22). The calculation results for models no. 1 and 2 are very similar and the only exception is pressure where the results for all models are distinguished. Hence further comparative analyses concern difference between the first two models and model no. 3.

The most significant differences are noticeable in the graphs of pressure (Figure 2) and its sensitivity (Figures 20 and 23(a)). It seems that the oldest model of boundary layer, i.e. model no. 1 is the least sensitive to the changes of parameters. It should be noted that the value of the particular sensitivity coefficient obtained for different boundary layers is usually of the same sign. In this case the pressure sensitivity coefficients are exceptional because the sensitivities for the first two boundary layer models have the same sign or if they have different signs their values do not significantly differ, whereas the results for model no. 3 have the opposite sign. The exception is the $\partial p / \partial \sigma_k$ coefficient for which very clear difference in the value is seen.

In the case of velocity, results obtained with the use of model no. 3 are different from the others in the region from $y \approx \pm 0.04$ m to the walls, but the calculation errors for this model are the smallest

in this area. However, in the middle of the channel cross section the calculation results from model no. 3 are the worst. The biggest differences between the graphs of the sensitivity coefficients for the three models are seen close to the wall. In this region for three parameters ($C_{\varepsilon 1}$, $C_{\varepsilon 2}$, C_{μ}), sensitivity decreases when the model is used and for the remaining two (σ_k , σ_{ε}) it increases. The graphs of the total influence of all parameters on the u_1 velocity, shown in Figure 23(b), is similar as the graph in Figure 3. The change of parameters can deteriorate the quality of solution at the middle of the channel and improve at the wall.

Another situation is for turbulence kinetic energy. The difference between calculation results obtained from different models is also the highest in the region from $y \approx \pm 0.04$ m to the walls, but the differences between calculation and measurements results are also in this region and they are the highest for model no. 3. As it was earlier noted bigger differences between measurements in wind tunnels and numerical results usually are for the bigger values of sensitivity coefficients and it is a fact that bigger sensitivity exists in the region of significant errors of calculations. The comparison of the sensitivity analysis results for three boundary layer models makes us see that for two parameters ($C_{\varepsilon 1}$, $C_{\varepsilon 2}$), sensitivity decreases when model no. 3 is used and for the remaining ones (C_{μ} , σ_k , σ_{ε}) it increases and the total influence of model parameters on solutions is when using model no. 3 for which the biggest calculation errors are obtained.

The largest errors in calculations of turbulence energy were obtained in the case of boundary layer model no. 3 for which the energy sensitivity is much larger than for the remaining models. The velocity calculation results are closer to the measurement results for model no. 3 than for other ones. Here the velocity sensitivities are lower for model no. 3 than models no. 1 and 2 as well. It confirms the dependence of the sensitivity to model parameters and quality of the numerical solutions. It is also seen that the problem of artificial simplification for the functions of the flow properties, which is described in the previous section does not exist at the comparison of the boundary layer models. Hence it can be noted that the dissipation is probably evaluated with higher error level for model no. 3 than for others because the increment of dissipation $\Delta\varepsilon$ taking into consideration the total influence of the model parameters is the highest for this model.

Unfortunately in this paper only three boundary layer models are researched and as it is seen in Figure 2 and the distributions of the sensitivity coefficients close to wall, these models are not perfect. It is impossible to affirm which of the methods is the best for the channel flow. The results obtained with use of models no. 1 and 2 are not different both for the flow properties and for the sensitivity coefficients. The velocity and probably turbulence viscosity are best modeled by model no. 3, but the remaining flow properties evaluated with the use of this model are burdened with higher errors than for other models. Therefore, the choice of the boundary layer model depends on which of flow properties are most important for the researcher. For the case when the aim of the calculation is the determination of the velocity field close to the wall without taking interest in remaining properties it can be noted that model no. 3 is the best, but for other situations this model is not perfect and model no. 1 or 2 should be preferably used.

5. CONCLUSIONS

In this paper the sensitivity analysis of a numerical solution to the parameters of the k - ε turbulence model for channel flow is made. The main conclusion is that numerical results obtained by using the k - ε turbulence model are very sensitive to the semi-empirical parameters: $C_{\varepsilon 1}$, $C_{\varepsilon 2}$, C_{μ} , σ_k and σ_{ε} . In the analysed problem, the dissipation rate of turbulence kinetic energy was found to be

the most sensitive to the parameters of the $k-\varepsilon$ model. Not only can this property be determined with a significant error in the calculations but it is also difficult to determine in tests. It seems that model verification should be carried out not only with regard to the flow velocity and its kinetic energy but also mainly by comparing calculation results with direct results of the turbulence dissipation rate tests.

All properties are mostly sensitive to the C_μ parameter, i.e. the coefficient defining the relation (comp. Equation (5)) between the kinetic energy and the dissipation rate on one side and turbulence viscosity on the other. Such a result confirms the importance of correct description of the turbulence viscosity in all problems of fluid mechanics and its large significance in obtaining the correct final result.

Only three models of the boundary layer are analysed in this paper. In the analysed problem of the channel flow, the use of more complicated and numerically time-consuming models does not improve the results. Obviously, in the case of problems using different, denser grids for the finite volume methods, this statement is likely to be false. It seems, however, that by introducing complex models the sensitivity of results to parameters does not decrease; in most cases it increases. This means that the calibration of parameters was made with the assumptions used with the standard $k-\varepsilon$ model for the case of the boundary layer, with a logarithmic velocity profile and the assumption of equilibrium between the energy production and the dissipation rate. Omitting these simplifications in more complicated models of turbulence and the boundary layer makes the properties more sensitive to the model parameters.

No analysis made for boundary layer model is perfect but it cannot be affirmed which of them is the best. The choice of the boundary layer model depends on which of the flow properties are most important for the researcher. For the case when the velocity or turbulence viscosity is the most important property model no. 3 can be used but to determine other properties model no. 1 or 2 seems to be better.

The presented analyses were performed at one set of the nominal parameter values which is the most commonly applied and for one exercise, i.e. the flow channel. In this case the function of flow properties with regard to the model parameters is nearly linear and the finite difference approach can be used to determine sensitivity coefficients. For the more complex problems, areas with very high gradients of flow properties with regard to the model parameters can exist. This means that the finite difference approach cannot be used. Additionally, the computer calculations of such problems probably should be made at other nominal parameter values. Moreover the sensitivity coefficients calculated at one nominal parameter value cannot be used for other model parameters, because they depend on model parameters, which may be seen in Figure 23.

It should be noted that the above conclusions concerning the results of the sensitivity analysis cannot be automatically used for other flow problems, but the calculation results presented in the author's papers [22, 23] confirm them nearly completely.

This paper presents calculation results that reveal that there is a correlation between the sensitivity coefficients and the quality of the results obtained. For the bigger values of sensitivity coefficients, the bigger differences between measurements in wind tunnels and numerical results should be expected. The model parameters are multipliers for the terms of Equations (1)–(5). The influence of these terms on the solution depends on the complexity of analysed problem. The high values of the terms cause significant influence of the parameter from this term on the results and the parameters from the small terms have smaller influence on these results. As the terms of the equations usually contain derivatives of flow properties with regard to coordinates, a similar relationship exists between the sensitivity of the solution to the model parameters and these derivatives. It means that

for one flow property the model parameter with high and small influences exists and, sometimes, the correlation between the quality of the solution and sensitivity coefficients cannot be seen. In such a situation the global influence can be calculated as it is proposed in the previous section.

Thus, it may be stated that the analysis of sensitivity coefficient fields allows checking solution reliability and indicating the areas of the greatest calculation difficulties. The sensitivity coefficient fields may also be used to determine areas where the model grid should be denser. The sensitivity analysis results may also be helpful in determination of the parameters for the k - ϵ model on the basis of wind tunnel tests made for various problems, which may increase the area of the k - ϵ turbulence model usability.

In this paper the sensitivity analysis of the channel flow to the parameters of the k - ϵ method have been performed using the finite difference approximation to the sensitivities coefficients. In the author's next paper the results of the use of the forward sensitivity analysis method to the channel flow will be presented. These results allow to compare both methods of determining the sensitivity coefficients.

Using each of the new methods for solving the main problem requires development of the sensitivity analysis program. An ideal solution would be if commercial programs for fluid mechanics had modules to analyse the sensitivity of results to the parameters of the turbulence model. This would enable the software users to check the result obtained with regard to the parameters assumed and concerning both the standard k - ϵ model and other turbulence models that comprise semi-empirical coefficients.

REFERENCES

1. Launder BE, Spalding DB. *Mathematical Models of Turbulence*. Academic Press: London, New York, 1972.
2. Launder BE, Spalding DB. The numerical computation of turbulent flows. *Computer Methods in Applied Mechanics and Engineering* 1974; **3**:269–289.
3. Hrenya CM, Bolio EJ, Chakrabarti D, Sinclair JL. Comparison of low Reynolds number k - ϵ turbulence models in predicting fully developed pipe flow. *Chemical Engineering Science* 1995; **50**(12):1923–1941.
4. Sarkar T, So RMC. A critical evaluation of near-wall two-equation models against direct numerical simulation data. *International Journal of Heat and Fluid Flow* 1997; **18**:197–208.
5. Prandtl L. Bericht über untersuchungen zur ausgebildeten turbulenz. *Zeitschrift für Angewandte Mathematik und Mechanik* 1925; **5**(2):136–139.
6. Kolmogorow AN. Equations of turbulent motion of an incompressible turbulent fluid. *Izvestiya Akademii Nauk SSSR* 1942; **VI**(1–2):56–58.
7. Bottema M. Turbulence closure model ‘constants’ and the problems of ‘inactive’ atmospheric turbulence. *Journal of Wind Engineering and Industrial Aerodynamics* 1997; **67**, **68**:897–908.
8. Comte-Bellot G, Corrsin S. The use of a contraction to improve the isotropy of grid-generated turbulence. *Journal of Fluid Mechanics* 1966; **25**:657–682.
9. Shih TH. An improved k - ϵ model near-wall turbulence and comparison with direct numerical simulation. *Report NASA TM 103221*, 1990.
10. Chen YS, Kim SW. Computation of turbulent flows using an extended k - ϵ turbulence closure model. *Report NASA CR-179204*, 1987.
11. Sarkar T, Sayer PG, Fraser SM. Flow simulation past axisymmetric bodies using four different turbulence models. *Applied Mathematical Modelling* 1997; **21**:783–792.
12. Batchelor GK. *The Theory of Homogeneous Turbulence*. Cambridge University Press: Cambridge, 1953.
13. Johansson AV. Engineering turbulence models and their development, with emphasis on explicit algebraic Reynolds stress models. *The Course of ‘Theories of Turbulence’*, organized by CISM, Udine, 2001.
14. Mohamed MS, Larue JC. The decay power law in grid generated turbulence. *Journal of Fluid Mechanics* 1990; **219**:195–214.
15. Shih TH, Liou WW, Shabbir A, Yang Z, Zhu J. A new k - ϵ eddy-viscosity model for high Reynolds number turbulent flows. *Computers and Fluids* 1995; **24**(3):227–238.

16. Wolfstein M. The velocity and temperature distribution of one-dimensional flow with turbulence augmentation and pressure gradient. *International Journal of Heat and Mass Transfer* 1969; **12**:301–318.
17. Kleiber M, Antúnez H, Hien TD, Kowalczyk P. *Parameter Sensitivity in Nonlinear Mechanics*. Wiley: New York, 1997.
18. Mohammadi B, Molho JI, Santiago JG. Incomplete sensitivities for the design of minimal dispersion fluidic channels. *Computer Methods in Applied Mechanics and Engineering* 2003; **192**:4131–4145.
19. Fernández MA, Moubachir M. Sensitivity analysis for an incompressible aeroelastic system. *Mathematical Model and Methods in Applied Sciences* 2002; **12**(8):1109–1130.
20. Błazik-Borowa E. The sensitivity analysis of CFD problems with using the $k-\varepsilon$ model on ‘constants’ of the turbulence model systems. *Journal of Transdisciplinary Systems Science* 2006; **11**(1)(Appendix):145–152.
21. Colin E, Etienne S, Pelletier D, Borggaard J. Application of a sensitivity equation method to turbulent flows with heat transfer. *International Journal of Thermal Sciences* 2005; **44**:1024–1038.
22. Błazik-Borowa E. The application of the sensitivity analysis of flow properties to parameters of the $k-\varepsilon$ method. *Proceedings of the 17th International Conference on Computer Methods in Mechanics*, Łódź-Spała, Poland, 2007; 91–92.
23. Błazik-Borowa E. The sensitivity analysis of the flow around a square cylinder to parameters of the $k-\varepsilon$ method. *Proceedings of 12th ICWE*, Cairns, Australia, 2007; **11**:1900–1926.
24. Błazik-Borowa E. The influence of input flow properties on the quality of the solution obtained with using of the $k-\varepsilon$ turbulence model. *Proceedings of Fifth Symposium on Environmental Effects on Buildings and People*, Kazimierz Dolny, Poland, 2007; 87–90.
25. Kim SW. A near-wall turbulence model and its application to fully developed turbulent channel and pipe flows. *Report NASA TM-101399*, 1988.
26. Viegas JR, Rubesin MW, Horstman CC. On the use of wall functions as boundary conditions for two-dimensional separated compressible flows. *AIAA-85-0180, AIAA 23rd Aerospace Sciences Meeting*, Reno, Nevada, 1985.